LETTER

ECOLOGY LETTERS   cnrs   WILEY

Intraspecific variation in species interactions promotes the feasibility of mutualistic assemblages

Blanca Arroyo-Correa[1] | **Pedro Jordano[1,2]** | **Ignasi Bartomeus[1]**

[1]Integrative Ecology Group, Estación Biológica de Doñana, EBD-CSIC, Sevilla, Spain

[2]Departamento de Biología Vegetal y Ecología, Facultad de Biología, Universidad de Sevilla, Sevilla, Spain

Correspondence
Blanca Arroyo-Correa, Integrative Ecology Group, Estación Biológica de Doñana, EBD-CSIC, Av. Américo Vespucio 26, Sevilla E-41092, Spain.
Email: blanca.arroyo@ebd.csic.es

Abstract
Patterns of resource use observed at the species level emerge from the way individuals exploit the range of available resources. Hence, accounting for interindividual differences in resource use, such as pollinator use by plants, is essential to advance our understanding of community assembly and persistence. By using finely resolved data on plant–pollinator interactions, we evaluated how interindividual plant variation in pollinator use scales up to affect community structure and dynamics. All co-occurring plant species comprised specialists interacting with proper subsets of pollinators that visited generalists, and differences in interaction patterns were driven by among-individual trait variation. Furthermore, the nested structure and feasibility of plant–pollinator communities were maximised at higher levels of interindividual plant variation in traits and pollinator use. Our study sheds light on how pervasive properties of community structure arise from individual-level processes and contributes to elucidate the importance of preserving intraspecific variation in traits and resource use within populations.

KEYWORDS
community persistence, individual specialisation, interindividual variation, mutualism, network stability, plant–pollinator interactions, pollination, population niche

INTRODUCTION

The niche concept has been pivotal to mainstream ecological research since its origins (Grinnell, 1917) and has permeated most theories aiming to explain biodiversity patterns. Traditionally, ecological niches have been described at the population level, treating conspecific individuals as functionally equivalent (Bolnick et al., 2011; Soulé & Stewart, 1970). However, niche variation within populations is a widespread phenomenon in such a way that many apparently generalised populations can be composed of individuals that greatly differ in the way they exploit the range of available resources (Van Valen, 1965; Violle et al., 2012). This among-individual variation might be a result of trait differences and environmental variation in resource availability across space and time. Although largely neglected, interindividual differences in resource use may have important consequences for population dynamics, species interactions, community structure and long-term coexistence (Barabás & D'Andrea, 2016; Bolnick et al., 2011; Costa-Pereira et al., 2019). Dismissing this level of analysis among individuals limits our understanding of the build-up processes that underpin complex ecological interaction networks.

The generalised interaction patterns we frequently document at the species level are often the outcome of nonrandom mixtures of specialists (i.e., individuals using small subsets of the population niche) and generalists (i.e., those using a large proportion of the entire population niche; Bolnick et al., 2003). Describing these complex patterns of resource use by multiple individuals

can be achieved using individual-based bipartite networks, where at least one of the two sets of nodes represent individuals and the links connecting them depict the interactions they establish (Guimarães, 2020; Olesen et al., 2010). The heuristic value of this individual-based approach has already revealed new insights into the ecological and evolutionary dynamics of species interactions (e.g., Dáttilo et al., 2014; Rodríguez-Rodríguez et al., 2017). For instance, among-individual variation in interaction patterns with pollinators is associated with plant individual's attractiveness, determined by plant phenotypic traits and neighbourhood composition (e.g., Arroyo-Correa et al., 2021; Dupont et al., 2014; Gómez & Perfectti, 2012). Unfortunately, empirical studies considering interindividual variation in interaction patterns usually focus on single species, giving little guidance as to how variance is distributed across multiple species and how it scales up to affect the community-level network structure and dynamics. Over the last decades, community ecology has classically used network theory to summarise and analyse ecological interactions at the species level (e.g., between plant and pollinator species; Ings et al., 2009; e.g., Bastolla et al., 2009; Vázquez et al., 2009). This approach often treats interindividual variation as noise, or as a black box, rather than as an important feature of ecological interactions. Moreover, we do not yet know how the properties of species-level interaction networks are affected by different patterns of among-individual variation in resource use (Figure 1, Clark et al., 2011).

Community-level mutualistic networks (i.e., species-based) usually exhibit nested patterns, wherein specialist species interact with a subset of those species with which generalist species also interact (Bascompte et al., 2003). More nested structures are predicted to have larger feasibility domains (i.e., to persist longer in time; Roberts, 1974; Goh, 1979; Saavedra et al., 2016). Feasibility domains describe the range of tolerated combinations of species demographic features, such as intrinsic growth rates, under which all species can have positive abundances (Rohr et al., 2014; Song et al., 2018). In the presence of an environmental perturbation, such as climate change or habitat loss, it is less likely that any of the species in a very feasible community will decline to extinction, as there is a wide range of conditions in which all species coexist stably. However, there is no evidence to date on how among-individual variation within mutualistic assemblages may affect communities' structure and persistence capacity. For instance, in a plant–pollinator community, an increase in the variability of pollinator use among plant individuals would be reflected in a higher number of pollinator species with which each plant species interacts (i.e., larger niche breadth), affecting the overlap in pollinator use among plant species, the overall structure of the interaction network and the predicted dynamics. Bridging the gap between community structure and dynamics becomes crucial under global change, as many populations are drastically decreasing in size and becoming more homogenous in traits (Sala et al., 2000; Tylianakis et al., 2008).
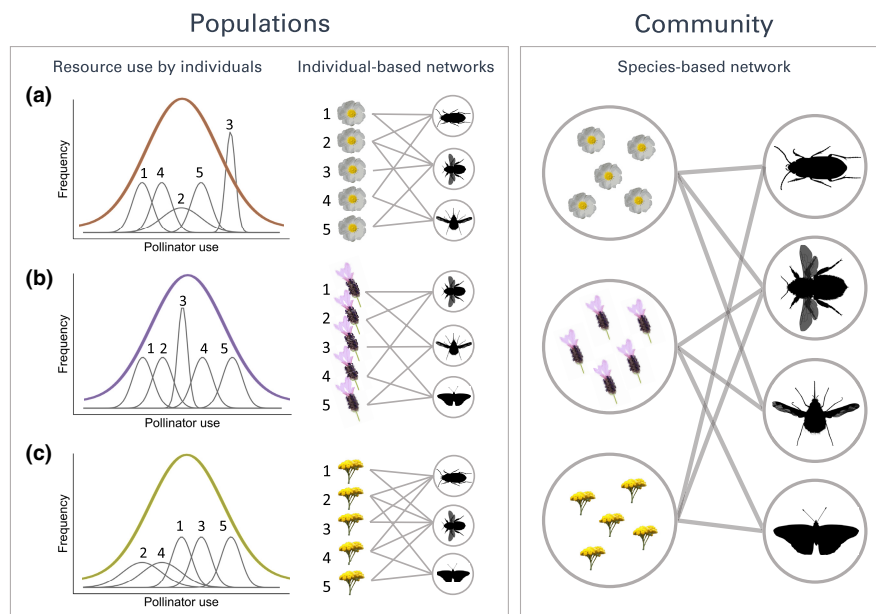
FIGURE 1 Upscaling from individual plant variation in pollinator use to the network of interactions among plant and pollinator species within communities. Within the populations of different plant species (a–c), individuals differ in how they use pollinator resources, leading to different levels of specificity in interaction patterns among plant individuals, which can be represented and analysed using individual-based networks. Because ecological interactions among species actually occur between individuals, these individual-based networks provide the building blocks for community-level networks (i.e., species-based networks). For the analysis at the community level, all these individuals' interactions within each plant species are usually aggregated (i.e., summed) in order to incorporate plant species-level interaction assemblages into the species-based network.

By integrating principles of niche theory and network approaches, we aimed to elucidate how community-level pervasive properties emerge as a result of interactions established by individuals and their consequences for community persistence. To that end, we used highly resolved data on plant–pollinator interactions collected at the plant individual level in Mediterranean shrublands. First, we evaluated how interindividual plant variation in interaction patterns is distributed across co-occurring species. The interaction patterns of each plant individual were estimated as the number of pollinator morphotypes used and the overlap in pollinator use with conspecific plants. Second, we assessed the drivers of this interindividual plant variation by analysing the contribution of plant attributes (i.e., phenotypic traits and neighbourhood characteristics). Third, we evaluated how interindividual variation in a key plant attribute, flower production, influences the structure (i.e., nestedness) and dynamics (i.e., feasibility) of community-level plant–pollinator networks. To disentangle the underlying mechanisms, we analysed the impact of interindividual variation in this plant attribute on the number of pollinator morphotypes used by plant species and the overlap in pollinator use among plant species, which in turn may affect the structure and dynamics of communities.

MATERIALS AND METHODS

Study site and sampling

The study was performed in Doñana National Park (37°0'29.736" N -6°30'24.919" W, 25 m a.s.l.), on the Atlantic coast of southwestern Spain. Our study area was located on the slopes of stabilised sand dunes, where the vegetation is composed mainly of Mediterranean sclerophyllous shrublands. We selected six 1200 m^2 plots, which were 300 m distance apart, that included 11 insect-pollinated shrub species (Figure S1). We used these six plots to capture locally variable environmental conditions and compositional variation in plant communities, as they differed in the relative abundance and density of shrub species and the depth of the water table.

We conducted surveys to record pollinator visitations in the study plots during the peak flowering period of the plant community (Figure S2, 164 days between early February and mid-July 2021). For each plant species, a variable number of plant individuals were selected (stratified random sampling, Figure S3) depending on local abundance within each plot, totalling 700 plant individuals (see Table S1 for sampling completeness). We performed weekly surveys on each flowering plant individual using video cameras (GoPro HERO7; GoPro Inc., Germany) together with visual censuses along random transects (Appendix S1.1). Pollinators were considered as all those insects landing on the flower and touching its reproductive structures and were identified at the species

level when possible (27.27%, Tables S2 and S3). We defined pollinator morphotypes as groups of pollinator specimens with very similar or identical morphology. We excluded two plant species from our analyses due to the extremely low abundance and the very early flowering period. Data obtained with video recordings were merged with those obtained with random transects by standardising all interaction data as the frequency of visits per minute to create an overall interaction dataset combining both methods (Appendix S1.2). An individual-based network for each plant species was built by creating an adjacency matrix A, where elements a_{ij} represent the frequency of interactions per time between the pollinator morphotype i and the plant individual j. Therefore, this network is only partially individual-based because we aimed to characterise the resource use (i.e., pollinator resources) by plant individuals within each species. To that end, we aggregated pollinator individuals at the morphotype level by summing all interactions established by pollinator individuals from the same morphotype. The individual-based network for each plant species was constructed by pooling data from all plots to include the complete range of environmental variation.

Plant attributes and topological roles

We estimated a series of intrinsic and extrinsic attributes for each individual plant. The intrinsic attributes included the plant height, total number of flowers produced along the season and flowering phenology, while the extrinsic attributes comprised the cover of conspecific and heterospecific neighbours expressed in terms of their relative abundance within a 1.5 m radius. This radius was identified as a good proxy for pollinator-mediated interactions (e.g., competition or facilitation; Ghazoul, 2006; Hegland, 2014). The neighbourhood composition was obtained with the help of drone flights (Appendix S1.3). We also calculated the flowering synchrony of a plant individual compared with conspecific and heterospecific neighbours within the plot following (Marquis, 1988; Appendix S1.4), which ranges from 1 (complete flowering overlap with neighbours) to 0 (no flowering overlap with neighbours). As we found strong evidence that plant height was correlated with the number of flowers produced (Pearson's $r = 0.57$, $p < 0.001$), we excluded plant height from analyses.

For each plant individual within the individual-based network of the plant species it belongs to, we calculated two topological metrics that reflect how interactions with pollinator morphotypes are assembled: degree and niche overlap ('bipartite' R package, Dormann et al., 2008). The degree is the total number of pollinator morphotypes used by a given plant individual and therefore represents the level of interaction specificity of this plant on pollinator use. The niche overlap represents the similarity between a given plant individual and all the other

conspecific plants in the use of pollinator morphotypes, and is estimated by calculating the average Bray–Curtis similarity (e.g., Gómez et al., 2010) in pollinator assemblage (i.e., the set of interacting pollinator partners) between this plant individual and every other plant in the population. It ranges between 0 and 1 and represents how quantitatively similar a given plant individual is in pollinator use (i.e., both in composition and abundance), compared with conspecifics (Appendix S1.5).

Statistical analyses

Interindividual plant variation in pollinator assemblage and topological roles

To explore variation among plant individuals and species in interaction patterns with pollinator morphotypes, we created an overall adjacency matrix by combining all plant individuals from all species, so each cell represents the frequency of interactions per time between a pollinator morphotype and a plant individual. We estimated the pairwise beta diversity of pollinator composition among plant individuals from all species as a Bray–Curtis distance in order to obtain a distance matrix among pairs of plant individuals (Anderson et al., 2011). Using this distance matrix, we tested whether plant species were similar in pollinator use (both in composition and abundance) using a permutational analysis of variance (PERMANOVA) and whether homogeneity of variances in pollinator composition differed among plant species using the PERMDISP2 procedure. To visualise differences and spread in beta-diversity measures among plant species, we used a nonparametric multidimensional scaling (NMDS). These analyses were done with the 'vegan' R package (Oksanen et al., 2022).

We further analysed the level of interindividual variation in pollinator use by assessing the range (coefficient of variation, CV) and distribution shape (skewness, S and kurtosis, K) of individuals' degree and overlap within each plant species (Appendix S1.7; Figure S5). Skewness quantifies the asymmetry of a given distribution (e.g., a skewed distribution indicates the dominance of extreme values in degree or overlap). Kurtosis quantifies the relative peakedness of a distribution and the relative density of its tails (e.g., a lower kurtosis reflects a more even distribution of values of degree or overlap). We analysed the deviation of the observed skewness and kurtosis values from those expected in a normal distribution ('moments' R package, Komsta & Novomestky, 2015). We also evaluated whether generalists contributed to enlarge the pollinator assemblage within a plant population composed of a mixture of specialist (lower degree) and generalist (higher degree) individuals. To do that, we estimated the nestedness (NODF, Almeida-Neto et al., 2008) of the individual-based network within each plant species (Appendix S1.8).

Correlates of interindividual plant variation in topological roles

We assessed the drivers of the interindividual variation in degree and overlap, for each plant species using linear models with degree and overlap as response variables and plant attributes as predictor variables. Individual-level metrics were log-transformed, and all predictor variables were scaled (ranging from 0 to 1) to allow meaningful comparisons. These models were fitted using the 'lme4' R package (Bates et al., 2015), and assumptions were tested with the 'Dharma' R package (Hartig, 2022). We assessed the relative contribution of each plant attribute in explaining interindividual variation in degree and overlap ('relaimpo' R package, Grömping, 2007).

Effects of interindividual variation on community-level network structure and dynamics

To analyse how interindividual plant variation is translated into community-level effects, we started by constructing an overall, individual-based network within the plant community by including all plant individuals from all species (Figure 2a). Then, we created a series of new resampled networks differing in interindividual variation in a key plant attribute, flower production, which generates networks differing in interindividual variation in interaction patterns with pollinators. Overall, the aim of our resampling procedure was to generate networks with high interindividual variation in flower production and networks with low interindividual variation in flower production. Networks with high interindividual variation were obtained by resampling plant individuals regardless of their flower production, capturing subsets of plant individuals that were heterogeneous in flower production. Meanwhile, networks with lower interindividual variation were obtained by resampling plant individuals only with low, medium and high flower production, capturing more internally homogeneous subsets of plant individuals.

To obtain resampled networks with high interindividual variation in flower production, we generated $N = 100$ networks by randomly sampling $m = 100$ plant individuals from the overall individual-based network, distributed among plant species proportional to their relative abundance. By doing so, we obtained a set of 100 resampled networks (i.e., 'random' set) that captures the observed interindividual variability in our community. Resampled networks with lower interindividual variability compared with the 'random' set were obtained by partitioning our individual-based interaction network into three equal networks, each containing one-third of the plant individuals. To define these terciles, plant individuals were arranged in order from lowest to highest flower production. We obtained three individual-based
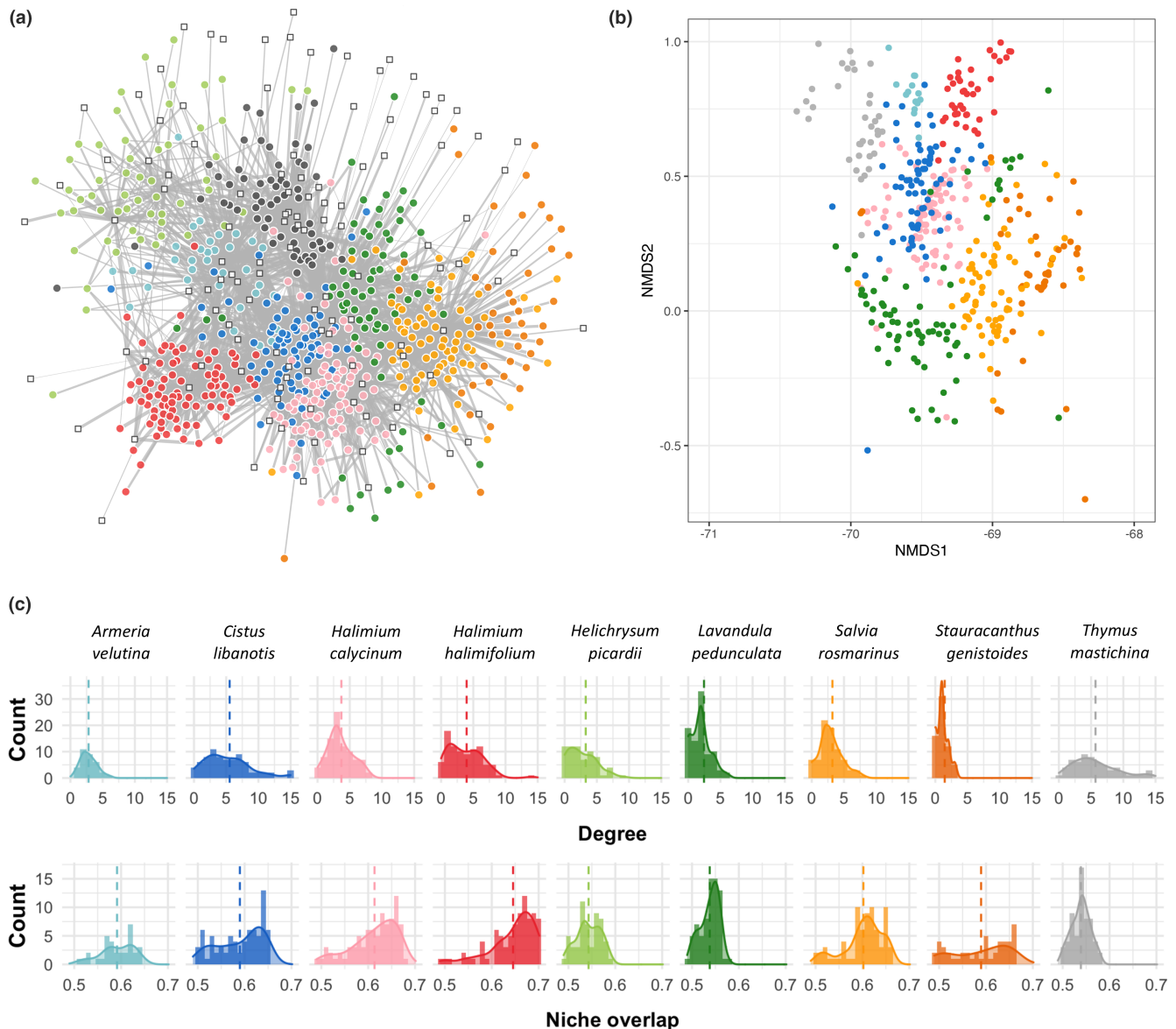
FIGURE 2 (a) Weighted bipartite network depicting interactions between plant individuals (circled nodes) and pollinator morphotypes (squared nodes) at the community. The links between nodes indicate flower visitation interactions while the width of the links refers to the strength of the interaction (i.e., number of interactions recorded). The layout of the network representation was created using an energy-minimisation algorithm. Different colours represent different plant species. (b) NMDS visualising beta diversity of pollinator composition among plant individuals. The spread of points describes differences in beta diversity of plant individuals of different plant species (colours). (c) Frequency distributions of degree (i.e., number of pollinator morphotypes used) and niche overlap (i.e., overlap in pollinator use with conspecifics) of plant individuals from different plant species (columns) in their individual-based networks. Dashed lines represent mean values. Shaded overlays are the density values (smoothed) for the distributions.

networks differing in flower production per plant individual: the 'lower tercile' (lowest flower production), the 'middle tercile' (medium flower production) and the 'upper tercile' (highest flower production) networks. As for the 'random' set, for each of these three individual-based networks, representing different levels of flower production, we generated $N = 100$ resampled networks by randomly sampling $m = 100$ plant individuals, distributing m among plant species proportional to their relative abundance. Hence, all this resampling procedure generates a set of networks with higher interindividual

variation in flower production ('random' set, capturing heterogeneous subsets of plant individuals) and lower interindividual variation ('lowest tercile', 'middle tercile' and 'upper tercile' sets, capturing more homogeneous subsets of plant individuals with low, medium and high flower production, respectively; Figure S7).

We transformed each of these resampled individual-based networks into a species-based binary network by summing the interactions established by plant individuals at the species level. Each species-based network is therefore represented as an adjacency matrix A, where

elements a_{ij} indicates the presence of an interaction (1 when an interaction occurs and 0 otherwise) between the pollinator morphotype i and the plant species j. As the theoretical background on the feasibility of mutualistic networks and its relationship with topology has currently only been developed for binary networks, we used the binary version of our species-based networks to estimate feasibility and nestedness. For each species-based network, we first calculated a nestedness measure (NODF; Almeida-Neto et al., 2008). Because NODF values can be influenced by the number of pollinator morphotypes included in the resampled networks, we illustrated these effects in Figure S8. Second, we calculated the feasibility conditions of each species-based network using a generalised Lotka–Volterra model to describe its population dynamics (Appendix S1.9). The range of feasible conditions (i.e., those leading to positive abundances for all co-occurring species) for a given community is known as the feasibility domain (Logofet, 1993). The larger the size of the feasibility domain, the larger the range of environmental conditions leading to a feasible community and the higher the tolerance of a community to random environmental variations (Rohr et al., 2014).

For each species-based network, we also estimated the average degree of plant species (i.e., number of pollinator morphotypes used) and the average overlap in pollinator use among plant species using the qualitative version of the Bray–Curtis similarity index (i.e., qualitative overlap of pollinator morphotypes among plant species, Appendix S1.6). The overlap among plant species was calculated as qualitative because our nestedness and feasibility estimations were based on binary networks. To test the effects of community size m on network properties, we repeated all the above procedures with different community sizes (Figure S9). Network- and species-level metrics were estimated using the 'bipartite' R package (Dormann et al., 2008). We tested the effects of the incorporation of interindividual variation on species-level interaction patterns and community properties using linear models. We set the degree of plant species and overlap among plant species in pollinator use, community-level nestedness (NODF) and feasibility as response variables, and the level of interindividual variation as the predictor variable. We considered two levels of interindividual variation in flower production, high variation for the 'random' set and low variation for the 'lower tercile', 'middle tercile' and 'upper tercile' sets.

To assess the hypothesis that interindividual variation in flower production ultimately determines community-level network structure and dynamics, we used a structural equation model (SEM), which allows us to quantify direct and indirect effects by linking multiple variables into a single causal framework (Lefcheck, 2016). We proposed a model in which the mean and variance of the number of flowers produced per individual may simultaneously affect plant species-level degree and overlap in pollinator use among plant species. Because the structure and dynamics of species-based plant–pollinator networks depend on how interactions among mutualistic partners are assembled, we included the plant species-level degree and the overlap in pollinator use among plant species as potential drivers of nestedness and feasibility. The model proposed was performed with a ratio of 36 data points per parameter to be estimated. We performed these analyses using the 'piecewiseSEM' R package (Lefcheck, 2016) and tested the overall fit based on Fisher's C statistics (Shipley, 2009).

RESULTS

Across the flowering season, we obtained 694.74 h of video recordings (1.48 ± 0.78 per plant individual, [mean $\pm SD$]) and performed approximately 1,000 h of visual censuses along random transects. We recorded a total of 34,775 interactions between 583 plant individuals (nine species) and 121 pollinator morphotypes (Figure 2a).

Interindividual plant variation in pollinator assemblage and topological roles

Beta-diversity of pollinator assemblages within plant species (i.e., dissimilarity in composition and abundance of pollinator morphotypes among conspecific plant individuals) ranged between 0.57 and 0.85 across plant species (0.72 ± 0.09 [mean $\pm SD$ across plant species]). We found moderate evidence that pollinator composition of plant individuals differed between plant species (PERMANOVA, $F = 40.65$, $R^2 = 0.36$, $p = 0.01$; Figure 2b) indicating that individuals were more similar to other individuals of the same species than to individuals of other species. The variance of beta diversity among plant individuals was very different between plant species (PERMDISP2, $F = 12.78$, $p < 0.001$).

We found variation among plant individuals in the role they played in the individual-based plant–pollinator network within the species they belong to. Across plant species, the coefficient of variation ranged between 44.64 and 63.68% for degree and 3.63 and 9.89% for overlap in pollinator use with conspecifics (Figure S4). We found strong evidence of kurtosis and skewness in the distributions of individual values of degree and overlap (Figure 2c; Figure S4). Specifically, we found a positive skewness in degree (i.e., number of pollinator morphotypes used) and a negative skewness in overlap for most plant species. Therefore, most plant species comprised a few plant individuals that were generalists (i.e., higher degree) and that interacted with a distinct pollinator assemblage compared with its population (i.e., lower overlap). Several plant species exhibited a low kurtosis in overlap and therefore comprised many individuals differing in overlap with conspecifics (Figure S4). We found evidence that specialist plant individuals (lower degree)

interacted with subsets of the pollinators visiting generalist plant individuals (higher degree; Table S4).

Correlates of interindividual plant variation in topological roles

Plant individuals' attributes affected their degree (i.e. number of pollinator morphotypes used) and overlap with conspecifics, but the direction and effect size highly depended on the plant species they belong to (see Tables S5 and S6 for the degree of evidence of effects). We found that the number of flowers produced positively affected the individual degree and overlap in most plant species. Therefore, those plant individuals that produced more flowers interacted with more pollinator morphotypes (higher degree) and shared more pollinators with conspecifics (higher overlap). For several plant species, the plant individuals' degree and overlap with conspecifics were also positively and negatively affected by conspecific and heterospecific flowering synchrony, respectively (see Figure S6 for effect sizes). Overall, variation in degree was mostly explained by flower production, while overlap in pollinator use with conspecifics was more explained by conspecific flowering synchrony (Table 1).

Effects of interindividual variation on community-level network structure and dynamics

In communities with higher interindividual variation (i.e., 'random set', capturing subsets of individuals heterogeneous in flower production), plant species overlapped less in pollinator use ($t = -26.81$, $p < 0.001$) despite interacting with the same number of pollinator

TABLE 1 Relative contribution of different plant attributes on the explained variance of plant individuals' degree (i.e., number of pollinator morphotypes used) and niche overlap (i.e., overlap in pollinator use with conspecifics). A mean $\pm$ *SD* percentage contribution was calculated for each plant attribute across plant species. These values were obtained as the average relative contribution of each predictor to the R^2 of the overall model over orderings of predictors

Plant attribute	Degree	Niche overlap
Number of flowers	45.98 ± 25.87	24.97 ± 21.55
Conspecific flowering synchrony	20.10 ± 18.46	36.03 ± 20.27
Heterospecific flowering synchrony	16.15 ± 11.85	21.03 ± 16.72
Conspecific neighbourhood cover	6.04 ± 6.72	6.49 ± 7.12
Heterospecific neighbourhood cover	11.74 ± 15.91	11.19 ± 21.47

morphotypes ($t = -1.13$, $p = 0.26$) compared with communities with low interindividual variation in flower production (i.e., 'lower tercile', 'middle tercile' and 'upper tercile sets', capturing more homogeneous subsets of individuals with low, medium and high flower production, respectively; Figure 3c). Besides, plant–pollinator communities with higher interindividual variation in flower production showed higher nestedness ($t = 3.51$, $p < 0.001$), (Figure 3b) and persistence capacity (i.e., feasibility, $t = 5.30$, $p < 0.001$, Figure 3a).

The structural equation model revealed that the mean number of flowers produced per plant individual and the interindividual variation in this plant attribute within a population influenced the feasibility of plant–pollinator communities through their effects on species-level interaction patterns. This model adequately represented the data and supported the hierarchical structure proposed (Fisher's C = 12.93, $p = 0.11$). We found strong evidence that the higher the flower production per plant individual, the higher the plant species-level degree and the overlap among plant species in pollinator use. Both plant species-level degree and among-species overlap decreased with interindividual variation in flower production. We also found evidence that nestedness increased with plant species-level degree and decreased with among-species overlap. The feasibility of plant–pollinator communities increased directly with plant species-level degree and decreased with among-species overlap in pollinator us, and was positively associated with nestedness (see Figure 4 for effect sizes). While the mean flower production per individual accounted for 69.89% of the total effects of individual flower production on the feasibility of communities, 30.11% were due to interindividual variation in this plant attribute (i.e., variance).

DISCUSSION

Ecological interactions established by individuals constitute the building blocks for the assembly of networks of interacting species. While in the last decades the importance of interindividual variability in natural populations has been widely recognised (Bolnick et al., 2003), little is known about how interacting assemblages of species within communities are influenced by this kind of variation. Using plant–pollinator communities as a study system, we showed that the underlying variation in plant attributes mediating the establishment of interactions with pollinators (e.g., flower production) translated into variation in interaction properties among plant individuals. Our results provide novel insights into how this variation can scale up to influence the emerging structure and the persistence capacity of species interaction networks and the mechanisms underlying these effects.

Plant populations of single species have been shown to exhibit high levels of partitioning in pollinator use by individuals (e.g., Arroyo-Correa et al., 2021; Dupont

FIGURE 3 Frequency distribution of community feasibility (a), nestedness (b), plant species-level degree (i.e., number of pollinator morphotypes used) and among-species overlap (i.e., overlap in pollinator used among plant species) (c) of species-based plant–pollinator networks. The 'random' set represents networks with high interindividual variation in flower production, capturing heterogeneous subsets of plant individuals. The 'lower tercile', 'middle tercile' and 'upper tercile' sets represent networks with lower interindividual variation in flower production, capturing more homogeneous subsets of plant individuals within the lower, middle and upper tercile of flower production, respectively. Within each set, we generated 100 species-based plant–pollinator networks by randomly selecting 100 plant individuals distributed among plant species proportionally to their relative abundance and summing the interactions established by these plant individuals at the species level. The vertical solid line within each distribution represents the mean value.

et al., 2014; Rodríguez-Rodríguez et al., 2017). Here, we extend this knowledge by exploring this interindividual partitioning simultaneously across multiple species. All plant species were composed of individuals that differed in pollinator use, and generalist plant individuals contributed to its population's pollinator assemblage by adding pollinator morphotypes that do not visit specialist plant individuals. These findings are in accordance with substantial evidence across different taxonomic groups that species of ecological generalists are in fact heterogeneous collections of relative generalist and specialist individuals (Bolnick et al., 2007; Van Valen, 1965).

To date, variation within species has been mostly assessed by estimating the variance or coefficient of variation across individuals (Benedetti-Cecchi, 2003; Start, 2019; Violle et al., 2011). We found that the coefficient of variation was higher for plant individuals' degree (i.e., number of pollinator morphotypes used) than for the overlap in pollinator use with conspecifics. Despite a large variation in degree, plant individuals within each species slightly differed in pollinator overlap, probably because they interacted with a common set of most abundant pollinator partners. Moreover, the skewness and kurtosis of individual roles' distribution within species can also reveal novel information about interindividual variation. The skewness and kurtosis of species functional traits' distributions explain a larger proportion of ecosystem functionality compared with the mean and

variance of these distributions (Gross et al., 2017; Gross et al., 2021). Across plant species, we showed the predominance of individuals interacting with larger numbers of pollinator morphotypes and overlapping less in pollinator use with conspecifics compared with all other individuals. As disassortative mutualistic interactions may affect population dynamics through highly skewed reproductive outcomes (Gómez & Perfectti, 2012), the observed patterns suggest that plant individuals may contribute differently to population persistence. This individual information is crucial to shift from a phenomenological to a mechanistic understanding of population dynamics, in which the system is predicted from the properties of its components (Plard et al., 2019).

Because sampling effort per plant individual was independent of the number of flowers produced, the effects of individual flower production on degree were produced by the distinctiveness in attraction between plant individuals differing in flower production. Besides, more synchronous plant individuals, both with conspecifics and heterospecifics, tended to show larger overlap in pollinator use with conspecifics and higher degree. Therefore, the patterns of interactions of a focal plant were not a function only of that plant's attributes but also of neighbouring plants' attributes. These results are in line with previous studies highlighting the importance of context-dependency of ecological interactions for single species (e.g., Arroyo-Correa et al., 2021; Dupont
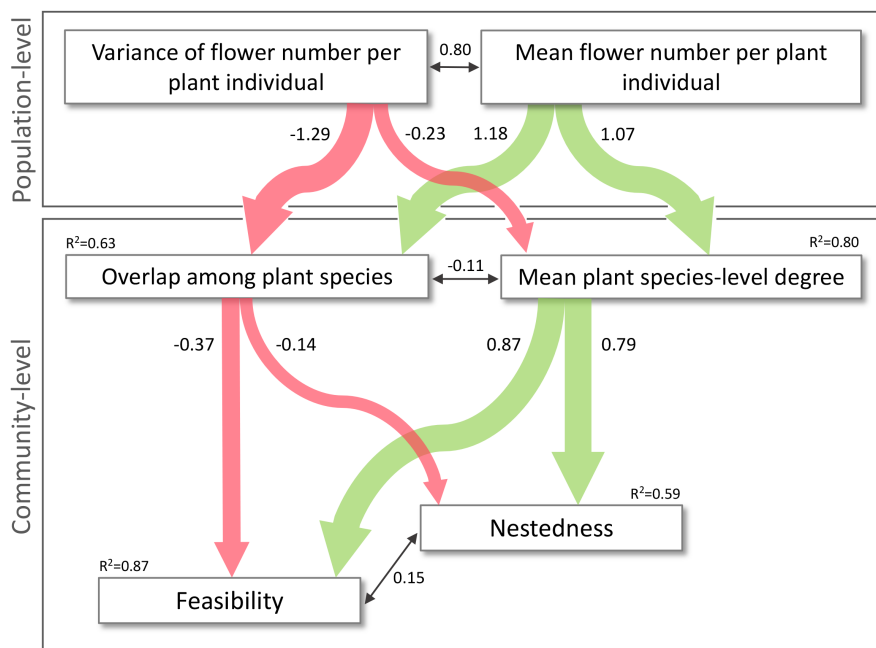
FIGURE 4 Structural equation model showing the effects of potential drivers of the structure (i.e., nestedness) and dynamics (i.e., feasibility) in plant–pollinator communities, starting from the mean flower production per plant individual and its variance within populations (i.e., interindividual variation). The mean plant species-level degree represents the mean number of pollinator morphotypes used by plant species and the overlap among plant species indicates the overlap in pollinator use among plant species. Standardised coefficients are presented as numbers next to arrows. Arrow widths are scaled to standardised coefficients. Green and red solid arrows indicate strong evidence ($P<0.001$) of positive and negative effects, respectively. Double black arrows indicate covariance. R^2 values show the proportion of explained variance in the response variables.

et al., 2014). In our multispecific approach, the contribution of the variation of different plant attributes on plant–pollinator interaction patterns was highly variable between plant species, suggesting that context dependency of interactions across species varies at small spatial scales. For example, while for some plant species, pollinator attraction was particularly affected by the number of flowers produced by plant individuals; for other co-occurring plant species, the flowering synchrony between individuals influenced more how they interacted with pollinators. Future research explicitly addressing the spatial processes generating patterns of interactions among individuals in a community context is needed (see Dupont et al., 2014; Pasquaretta et al., 2017 for single species).

It has been long acknowledged that interspecific variation influences community assembly, stability and ecosystem services (Cardinale et al., 2002; Tilman et al., 1998), but much less attention has been paid to the ecological importance of intraspecific variation. Trait variation within species can be as large as the trait variation across species (Albert et al., 2010), and consequently, intraspecific variation may influence ecosystem structure and function as much as variation among species (Des Roches et al., 2018). The incorporation of interindividual variation in an important plant attribute, flower production, within plant communities greatly reduced the overlap in pollinator use among plant species.

Interindividual variation in flower production was partially influenced by variation in plant size, although it was also probably affected by water availability or genetic predisposition, among other factors. Regardless of the causes of interindividual variation in flower production, this result provides evidence on how intraspecific variation can shift a population's position along the niche continuum, shaping the patterns of species overlap in resource use, and potentially resulting in facilitative or competitive relationships among these species (Start, 2019). By controlling the relative importance of niche and neutral processes, which greatly depends on the among-species overlap in resource use, intraspecific variation might influence community dynamics (Gravel et al., 2006).

Through its effects on plant species-level degree (i.e., number of pollinator morphotypes used by plant species) and among-species overlap, interindividual variation scaled up to influence nested patterns and persistence capacity of plant–pollinator communities. One of the mechanisms underlying the effect of interindividual variation in flower production on community-level nestedness was related to the effects on plant species-level degree. The higher the interindividual variation in flower production, the higher the number of pollinator morphotypes used by plant species, and the higher the nestedness of plant–pollinator communities (Figure S8). It has been previously demonstrated

that there is a positive association between the structure and dynamics of communities in mutualistic assemblages (Saavedra et al., 2016). Our results provide insights into how this association between network topology and feasibility emerges. We found that community feasibility was maximised with high plant species-level degree and low overlap among species. Whereas the number of flowers produced per individual largely increased community feasibility by increasing plant species-level degree, we also found that interindividual variation had an important role in promoting feasibility by lessening the overlap in pollinator use among plant species. Lower among-species niche overlap meant a broader range of conditions leading to coexistence, consistent with earlier results (Barabás et al., 2014). Communities composed of variable populations were on average 28% more feasible than communities comprising similar individuals, especially when those had low flower production. Hence, these results support the idea that any process homogenising traits (e.g., disturbances or management actions such as fires or clear-cuts) throughout populations may strongly affect community persistence. Although we are not yet able to incorporate theoretically the effect of individual-level variation in community dynamics, future work should explicitly address how nonrandom mixtures of generalist and specialist individuals composing populations may affect the predicted dynamics of communities. Besides, considering that interaction strengths could influence community persistence outcomes, we would need prospective research that seeks to develop a theoretical basis for incorporating quantitative interaction data into the estimation of mutualistic communities' feasibility (Grilli et al., 2017).

Intraspecific variation is both the product and the foundation of evolutionary and ecological processes. Our study provides an in-depth understanding of the interplay between individual trait variation, individual interaction variation, the emerging species' interaction patterns and their subsequent effects on community structure and dynamics. By taking into account the direct effects of interindividual trait variation on community feasibility, we highlight the importance of preserving within-population intraspecific variation in ecological interactions. Current conservation efforts, which are usually focused on species, overlook intraspecific variation and its corresponding ecological effects (Angelini et al., 2011; Power et al., 1996). However, variation within species is particularly subject to human impacts through declines in population genetic diversity and local extirpation (Miraldo et al., 2016; Moran et al., 2016; Palkovacs et al., 2012). In fact, current extinction rates of populations are orders of magnitude greater than extinction rates of species (Ceballos et al., 2015; Leclère et al., 2020). Thus, a deep comprehension of the ecological consequences of intraspecific variation is essential for predicting how rapid and widespread changes in diversity within species will impact communities and ecosystems.

PEER REVIEW
The peer review history for this article is available at https://publons.com/publon/10.1111/ele.14163.

DATA AVAILABILITY STATEMENT
Data and R code generated for this study are available at Zenodo Digital Repository (https://doi.org/10.5281/zenodo.7326843, Arroyo-Correa et al., 2022) and the GitHub repository (https://github.com/BlancaAC).

ORCID

Blanca Arroyo-Correa https://orcid.org/0000-0002-9402-3013
Pedro Jordano https://orcid.org/0000-0003-2142-9116
Ignasi Bartomeus https://orcid.org/0000-0001-7893-4389

REFERENCES

Albert, C.H., Thuiller, W., Yoccoz, N.G., Douzet, R., Aubert, S. & Lavorel, S. (2010) A multi-trait approach reveals the structure and the relative importance of intra-vs. interspecific variability in plant traits. *Functional Ecology*, 24(6), 1192–1201.

Almeida-Neto, M., Guimaraes, P., Guimaraes, P.R., Jr., Loyola, R.D. & Ulrich, W. (2008) A consistent metric for nestedness analysis in ecological systems: reconciling concept and measurement. *Oikos*, 117(8), 1227–1239.

Anderson, M.J., Crist, T.O., Chase, J.M., Vellend, M., Inouye, B.D., Freestone, A.L. et al. (2011) Navigating the multiple meanings of β diversity: a roadmap for the practicing ecologist. *Ecology Letters*, 14(1), 19–28.

Angelini, C., Altieri, A.H., Silliman, B.R. & Bertness, M.D. (2011) Interactions among foundation species and their consequences for community organization, biodiversity, and conservation. *Bioscience*, 61(10), 782–789.

Arroyo-Correa, B., Bartomeus, I. & Jordano, P. (2021) Individual-based plant–pollinator networks are structured by phenotypic and microsite plant traits. *Journal of Ecology*, 109(8), 2832–2844.

Arroyo-Correa, B., Jordano, P. & Bartomeus, I. (2022) Intraspecific variation in species interactions promotes the feasibility of mutualistic assemblages [data set]. *Zenodo*. Available from: https://doi.org/10.5281/zenodo.7326843

Barabás, G. & D'Andrea, R. (2016) The effect of intraspecific variation and heritability on community pattern and robustness. *Ecology Letters*, 19(8), 977–986.

Barabás, G., Pásztor, L., Meszéna, G. & Ostling, A. (2014) Sensitivity analysis of coexistence in ecological communities: theory and application. *Ecology Letters*, 17(12), 1479–1494.

Bascompte, J., Jordano, P., Melián, C.J. & Olesen, J.M. (2003) The nested assembly of plant–animal mutualistic networks. *PNAS*, 100(16), 9383–9387.

Bastolla, U., Fortuna, M.A., Pascual-García, A., Ferrera, A., Luque, B. & Bascompte, J. (2009) The architecture of mutualistic networks minimizes competition and increases biodiversity. *Nature*, 458(7241), 1018–1020.

Bates, D., Mächler, M., Bolker, B. & Walker, S. (2015) Fitting linear mixed-effects models using lme4. *Journal of Statistical Software*, 67(1), 1–48.

Benedetti-Cecchi, L. (2003) The importance of the variance around the mean effect size of ecological processes. *Ecology*, 84(9), 2335–2346.

Bolnick, D.I., Amarasekare, P., Araújo, M.S., Bürger, R., Levine, J.M., Novak, M. et al. (2011) Why intraspecific trait variation matters in community ecology. *Trends in Ecology & Evolution*, 26(4), 183–192.

Bolnick, D.I., Svanbäck, R., Araújo, M.S. & Persson, L. (2007) Comparative support for the niche variation hypothesis that more generalized populations also are more heterogeneous. *PNAS*, 104(24), 10075–10079.

Bolnick, D.I., Svanbäck, R., Fordyce, J.A., Yang, L.H., Davis, J.M., Hulsey, C.D. et al. (2003) The ecology of individuals: incidence and implications of individual specialization. *The American Naturalist*, 161(1), 1–28.

Cardinale, B.J., Palmer, M.A. & Collins, S.L. (2002) Species diversity enhances ecosystem functioning through interspecific facilitation. *Nature*, 415(6870), 426–429.

Ceballos, G., Ehrlich, P.R., Barnosky, A.D., García, A., Pringle, R.M. & Palmer, T.M. (2015) Accelerated modern human–induced species losses: entering the sixth mass extinction. *Science Advances*, 1(5), e1400253.

Clark, J.S., Bell, D.M., Hersh, M.H., Kwit, M.C., Moran, E., Salk, C. et al. (2011) Individual-scale variation, species-scale differences: inference needed to understand diversity. *Ecology Letters*, 14(12), 1273–1287.

Costa-Pereira, R., Araújo, M.S., Souza, F.L. & Ingram, T. (2019) Competition and resource breadth shape niche variation and overlap in multiple trophic dimensions. *Proceedings of the Royal Society B*, 286(1902), 20190369.

Dáttilo, W., Fagundes, R., Gurka, C.A., Silva, M.S., Vieira, M.C., Izzo, T.J. et al. (2014) Individual-based ant-plant networks: diurnal-nocturnal structure and species-area relationship. *PLoS One*, 9(6), e99838.

Des Roches, S., Post, D.M., Turley, N.E., Bailey, J.K., Hendry, A.P., Kinnison, M.T. et al. (2018) The ecological importance of intraspecific variation. *Nature Ecology and Evolution*, 2(1), 57–64.

Dormann, C.F., Gruber, B. & Fründ, J. (2008) Introducing the bipartite package: analysing ecological networks. *R News*, 8(2), 8–11.

Dupont, Y.L., Trøjelsgaard, K., Hagen, M., Henriksen, M.V., Olesen, J.M., Pedersen, N.M. et al. (2014) Spatial structure of an individual-based plant–pollinator network. *Oikos*, 123(11), 1301–1310.

Ghazoul, J. (2006) Floral diversity and the facilitation of pollination. *Journal of Ecology*, 94, 295–304.

Goh, B.S. (1979) Stability in models of mutualism. *The American Naturalist*, 113(2), 261–275.

Gómez, J.M., Abdelaziz, M., Lorite, J., Jesús Muñoz-Pajares, A. & Perfectti, F. (2010) Changes in pollinator fauna cause spatial variation in pollen limitation. *Journal of Ecology*, 98(5), 1243–1252.

Gómez, J.M. & Perfectti, F. (2012) Fitness consequences of centrality in mutualistic individual-based networks. *Proceedings of the Royal Society B*, 279(1734), 1754–1760.

Gravel, D., Canham, C.D., Beaudet, M. & Messier, C. (2006) Reconciling niche and neutrality: the continuum hypothesis. *Ecology Letters*, 9(4), 399–409.

Grilli, J., Adorisio, M., Suweis, S., Barabás, G., Banavar, J.R., Allesina, S. et al. (2017) Feasibility and coexistence of large ecological communities. *Nature Communications*, 8(1), 1–8.

Grinnell, J. (1917) The niche-relationships of the California thrasher. *The Auk*, 34(4), 427–433.

Grömping, U. (2007) Relative importance for linear regression in R: the package relaimpo. *Journal of Statistical Software*, 17, 1–27.

Gross, N., Bagousse-Pinguet, Y.L., Liancourt, P., Berdugo, M., Gotelli, N.J. & Maestre, F.T. (2017) Functional trait diversity maximizes ecosystem multifunctionality. *Nature Ecology and Evolution*, 1(5), 1–9.

Gross, N., Le Bagousse-Pinguet, Y., Liancourt, P., Saiz, H., Violle, C. & Munoz, F. (2021) Unveiling ecological assembly rules from commonalities in trait distributions. *Ecology Letters*, 24(8), 1668–1680.

Guimarães, P.R. (2020) The structure of ecological networks across levels of organization. *Annual Review of Ecology, Evolution, and Systematics*, 51(1), 433–460.

Hartig, F. (2022) DHARMa: residual diagnostics for hierarchical (multi-level/mixed) regression models. R package version 0.4.6.

Hegland, S.J. (2014) Floral neighbourhood effects on pollination success in red clover are scale-dependent. *Functional Ecology*, 28(3), 561–568.

Ings, T.C., Montoya, J.M., Bascompte, J., Blüthgen, N., Brown, L., Dormann, C.F. et al. (2009) Ecological networks–beyond food webs. *The Journal of Animal Ecology*, 78(1), 253–269.

Komsta, L. & Novomestky, F. (2015) Moments: moments, cumulants, skewness, kurtosis and related tests. R package version 0.14.

Leclère, D., Obersteiner, M., Barrett, M., Butchart, S.H., Chaudhary, A., De Palma, A. et al. (2020) Bending the curve of terrestrial

biodiversity needs an integrated strategy. *Nature*, 585(7826), 551–556.

Lefcheck, J.S. (2016) piecewiseSEM: piecewise structural equation modelling in r for ecology, evolution, and systematics. *Methods in Ecology and Evolution*, 7(5), 573–579.

Logofet, D.O. (1993) *Matrices and graphs: stability problems in mathematical ecology*. Boca Raton, FL: CRC press.

Marquis, R.J. (1988) Phenological variation in the neotropical understory shrub piper arielanum: causes and consequences. *Ecology*, 69(5), 1552–1565.

Miraldo, A., Li, S., Borregaard, M.K., Flórez-Rodríguez, A., Gopalakrishnan, S., Rizvanovic, M. et al. (2016) An Anthropocene map of genetic diversity. *Science*, 353(6307), 1532–1535.

Moran, E.V., Hartig, F. & Bell, D.M. (2016) Intraspecific trait variation across scales: implications for understanding global change responses. *Global Change Biology*, 22(1), 137–150.

Oksanen, J.A.R.I., Blanchet, F.G., Friendly, M., Kindt, R., Legendre, P., McGlinn, D. et al. (2022) Vegan: community ecology package. R package version 2.5–7.

Olesen, J.M., Dupont, Y.L., O'Gorman, E., Ings, T.C., Layer, K., Melian, C.J. et al. (2010) From Broadstone to Zackenberg: space, time and hierarchies in ecological networks. *Advances in Ecological Research*, 42, 1.

Palkovacs, E.P., Kinnison, M.T., Correa, C., Dalton, C.M. & Hendry, A.P. (2012) Fates beyond traits: ecological consequences of human-induced trait change. *Evolutionary Applications*, 5(2), 183–191.

Pasquaretta, C., Jeanson, R., Andalo, C., Chittka, L. & Lihoreau, M. (2017) Analysing plant-pollinator interactions with spatial movement networks. *Ecological Entomology*, 42(S1), 4–17.

Plard, F., Fay, R., Kéry, M., Cohas, A. & Schaub, M. (2019) Integrated population models: powerful methods to embed individual processes in population dynamics models. *Ecology*, 100(6), e02715.

Power, M.E., Tilman, D., Estes, J.A., Menge, B.A., Bond, W.J., Mills, L.S. et al. (1996) Challenges in the quest for keystones: identifying keystone species is difficult—but essential to understanding how loss of species will affect ecosystems. *Bioscience*, 46(8), 609–620.

Roberts, A. (1974) The stability of a feasible random ecosystem. *Nature*, 251(5476), 607–608.

Rodríguez-Rodríguez, M.C., Jordano, P. & Valido, A. (2017) Functional consequences of plant-animal interactions along the mutualism-antagonism gradient. *Ecology*, 98(5), 1266–1276.

Rohr, R.P., Saavedra, S. & Bascompte, J. (2014) On the structural stability of mutualistic systems. *Science*, 345(6195), 1253497.

Saavedra, S., Rohr, R.P., Olesen, J.M. & Bascompte, J. (2016) Nested species interactions promote feasibility over stability during the assembly of a pollinator community. *Ecology and Evolution*, 6(4), 997–1007.

Sala, O.E., Stuart Chapin, F.I.I.I., Armesto, J.J., Berlow, E., Bloomfield, J., Dirzo, R. et al. (2000) Global biodiversity scenarios for the year 2100. *Science*, 287(5459), 1770–1774.

Shipley, B. (2009) Confirmatory path analysis in a generalized multilevel context. *Ecology*, 90(2), 363–368.

Song, C., Rohr, R.P. & Saavedra, S. (2018) A guideline to study the feasibility domain of multi-trophic and changing ecological communities. *Journal of Theoretical Biology*, 450, 30–36.

Soulé, M. & Stewart, B.R. (1970) The "niche-variation" hypothesis: a test and alternatives. *The American Naturalist*, 104(935), 85–97.

Start, D. (2019) Individual and population differences shape species interactions and natural selection. *The American Naturalist*, 194(2), 183–193.

Tilman, D., Lehman, C.L. & Bristow, C.E. (1998) Diversity-stability relationships: statistical inevitability or ecological consequence? *The American Naturalist*, 151(3), 277–282.

Tylianakis, J.M., Didham, R.K., Bascompte, J. & Wardle, D.A. (2008) Global change and species interactions in terrestrial ecosystems. *Ecology Letters*, 11(12), 1351–1363.

Van Valen, L. (1965) Morphological variation and width of ecological niche. *The American Naturalist*, 99(908), 377–390.

Vázquez, D.P., Blüthgen, N., Cagnolo, L. & Chacoff, N.P. (2009) Uniting pattern and process in plant–animal mutualistic networks: a review. *Annals of Botany*, 103(9), 1445–1457.

Violle, C., Enquist, B.J., McGill, B.J., Jiang, L.I.N., Albert, C.H., Hulshof, C. et al. (2012) The return of the variance: intraspecific variability in community ecology. *Trends in Ecology & Evolution*, 27(4), 244–252.

Violle, C., Nemergut, D.R., Pu, Z. & Jiang, L. (2011) Phylogenetic limiting similarity and competitive exclusion. *Ecology Letters*, 14(8), 782–787.

SUPPORTING INFORMATION

Additional supporting information can be found online in the Supporting Information section at the end of this article.

Supporting Information

Intraspecific variation in species interactions promotes the feasibility of mutualistic assemblages

Blanca Arroyo-Correa[1], Pedro Jordano[1,2], Ignasi Bartomeus[1]

[1] *Dept. Integrative Ecology, Estación Biológica de Doñana, EBD-CSIC, Av. Américo Vespucio 26, Sevilla E-41092, Spain*

[2] *Dept. Biología Vegetal y Ecología, Universidad de Sevilla, Av. Reina Mercedes, E-41012, Sevilla, Spain*

Appendix S1. Supplementary methods

S1.1 Sampling of plant-pollinator interactions

The transects consisted of approximately 60 min random walks passing through all flowering plants in each plot while annotating the identity and frequency of visits of pollinator morphotypes on plant individuals. Each plant individual was video-recorded for 30 min each week during its flowering phenophase and therefore, the total time of video recording per plant individual along the season varied depending on the total number of weeks with flowers. As we set a fixed time per plant individual each week, the sampling effort for video recordings did not depend on the number of flowers displayed per individual in each sampling week. Video recordings per plant individual were carried out at different times during the time period with open flowers (8:30 to 16:30), spanning different sampling days. This sampling period encompassed the time of the day where the maximum activity of flower visitors to the plant community occurs. Video cameras were placed approximately 30cm away from the plant and were set up at varying heights in each of the different surveys to account for variation in floral displays. Video recordings were processed to annotate the identity of pollinator morphotype visiting all the flowers in view and the number of times they interacted with those flowers (i.e., frequency of visits). To facilitate pollinators' identification, a single representative specimen of most pollinator morphotypes present in the study site was captured in the field, identified, and vouchered at Estación Biológica de Doñana.

S1.2 Interaction data standardization and merging

For each plant individual, visits by pollinator morphotypes obtained with video recordings

were standardized per time (i.e., number of visits per minute) taking into account the total duration of video recordings in that plant individual. Using information from video recordings, we calculated the time period (minutes) needed to record one interaction per m^2 of a plant individual from a given species and plot. As we did not establish a fixed time along random transects, we used this value to estimate the frequency of visits per minute in each plant individual from transect data. The time spent on a focal plant individual to record the number of visits observed along transects was calculated by multiplying the total visits recorded in transects by all pollinator morphotypes on that plant, the individual plant size (m^2) and the mean time needed (minutes) to record one visit per m^2 in an individual of that plant species. After obtaining the time needed for each focal plant individual, we divided the number of visits per pollinator morphotype by this period of time to obtain the number of visits per minute. Finally, to merge the interaction data obtained with video recordings and random transects, we summed both interaction matrices (plant individuals x pollinator morphotypes) containing data on frequency of visits per time.

S1.3 Drone flights and neighborhood estimation

Plant size and spatial location of each plant individual were obtained using aerial images of the study site, with which we generated an orthomosaic together with a 3D digital surface model using the Pix4D software (Pix4D SA, Prilly, Switzerland). Aerial images were acquired with a flight height of 70 m and a pixel size of 1.71 cm using a Phantom 4 RTK drone (DJI Sciences and Technologies Ltd, China). The information derived from the aerial images was validated using a high-accuracy GNSS handheld (Trimble Geo 7x, Trimble Inc., Wesminster, USA) to register the spatial location. We used the orthomosaic to digitize all selected individual plants in the study site (n= 700). The polygon layer generated was used to

establish buffers of 1.5m around each individual plant to estimate the intraspecific and interspecific neighborhood cover. We estimated the cover of conspecific and heterospecific neighbors within a 1.5m radius around each of the sampled plant individuals. We measured the cover of all neighbors growing within this radius, regardless of whether these neighbors were marked and sampled. Therefore, our neighborhood estimation for each sampled plant individual was not dependent on the number of plant individuals sampled per each species because it was a variable describing the entire composition of neighbors observed in the field within a 1.5m radius. In addition, the sampled plant individuals of each species were selected so that they could not share neighbors within the established radius. Hence, plant individuals of the same species were independent in terms of the ecological context (i.e., the neighborhood surroundings) in which they were found.

S1.4 Flowering synchronization index

For each individual plant within the community, we estimated the flowering phenology by counting the number of flowers every week during the entire flowering peak season. We calculated the flowering synchronization level by modifying the index proposed by Marquis (1988) as follows:

$$S_i = \frac{\sum_{t=0}^{n} \left(\frac{x_t}{\sum_{t=0}^{n} x_t} \right)(p_t)}{n}$$

where S_i is the mean flowering synchronization level of individual i, averaged over n censuses carried out during the peak flowering season, x_t is the number of open flowers on individual i at time t, $\frac{x_t}{\sum_{t=0}^{n} x_t}$ is the proportion of open flowers on individual i of the total number of open flowers in that individual during the peak flowering season, n is the number

of censuses during the peak flowering season, and p_t is the proportion of individuals in flower at time t. Using this index we calculated the flowering synchrony of an individual plant within its species (i.e., p_t is the proportion of conspecific individuals in flower at time t in the plot) and with other species (i.e., p_t is the proportion of heterospecific individuals in flower at time t in the plot). Therefore, conspecific flowering synchrony was calculated by including only conspecific plant individuals in the estimation, while heterospecific synchrony was estimated by incorporating only heterospecific plants.

S1.5 Quantitative Bray-Curtis similarity index

To calculate the quantitative overlap (i.e., similarity) between a given plant individual and all the other conspecific plants in the use of pollinator morphotypes, we estimated the average Bray-Curtis similarity in pollinator assemblage (i.e., the set of interacting pollinator partners) between this plant individual and every other plant in the population. For two given plant individuals (i and i'), we followed:

$$BC_{ii'} = \frac{\sum_{j=1}^{J} | n_{ij} + n_{i'j} |}{n_{i+} + n_{i'+}}$$

where n_{ij} and $n_{i'j}$ are the abundance of pollinator morphotype j recorded in plant individuals i and i', respectively; and n_{i+} and $n_{i'+}$ are the total abundance of pollinator morphotypes in plant individuals i and i', respectively. This quantitative Bray-Curtis similarity index represents how quantitatively similar a given plant individual is in pollinator use (i.e., both in composition and abundance), compared to conspecifics. It ranges from 0 (if both plant individuals have absolutely no shared pollinator morphotypes) to 1 (if both plant individuals share the same number of pollinator morphotypes, at the same abundance). We used this

5

similarity index because it is expressed in a biologically-meaningful way that facilitates the interpretation of the compositional similarity between two different plant individuals, based on both the identity and the abundance of pollinator morphotypes visiting them.

S1.6 Qualitative Bray-Curtis similarity index (i.e., Sorensen index)

We calculated the qualitative overlap (i.e., similarity) between two given plant species (i and i') in the use of pollinator morphotypes as follows:

$$S_{ii'} = \frac{2 * C_{ii'}}{2 * C_{ii'} + S_i + S_{i'}}$$

where $C_{ii'}$ is the number of pollinator morphotypes recorded on both plant species, S_i is the number of pollinator morphotypes recorded in plant species i, and $S_{i'}$ is the number of pollinator morphotypes recorded in plant species i'. This index represents how qualitatively similar a given plant species is in pollinator use (i.e., in composition), compared to other plant species. It ranges from 0 (if both plant species do not share any pollinator morphotypes) to 1 (if both plant species share exactly the same pollinator morphotypes).

S1.7 Coefficient of variation, skewness and kurtosis of plant individuals' topological roles

We analyzed how the coefficient of variation (CV), skewness (S) and kurtosis (K) of the degree and niche overlap of plant individuals within each species varies over an increasing population size (i.e., number of individuals composing the individual-based network of the species they belong to). To do that, we generated individual-based plant-pollinator networks containing different numbers of nodes in the plant-mode (i.e., plant individuals) and their interactions with pollinator morphotypes. For each plant species we resampled a

6

total of N (n m), where *n* is the total number of plant individuals within a species (Table S1) and *m* is the number of plant individuals included in the resampled individual-based network for that plant species. For each *n* between two up to the total number of sampled individuals per plant species, we resampled N=100 combinations without replacement. Therefore, within each plant species and for each *n* we had 100 resampled individual-based networks with interactions between *n* randomly selected plant individuals and the pollinator morphotypes visiting them.

For each plant individual in its individual-based network, we estimated the same topological metrics as stated above and calculated the *CV*, *S* and *K* of these metrics within each resampled network. By assessing the standard deviation of *CV*, *S* and *K* across random samplings of different numbers of individuals within the population, we aimed to estimate the population size at which *CV*, *S* and *K* in degree and overlap stabilized. We considered that the *CV*, *S* and *K* ceased to accumulate within a population by setting an arbitrary cutoff for the standard deviation of this CV at 10% in order to allow comparisons between metrics. CV stabilized at 54.20 ± 28.30 individuals for degree [mean ± SD] and 2.00 ± 0.00 for overlap, skewness at 2.00 ± 0.00 for degree and 53.30 ± 27.70 for overlap, and kurtosis at 2.00 ± 0.00 for degree and 3.00 ± 0.00 for overlap (Fig. S5). As these values stabilized at a smaller number of individuals than those in our sample size for each plant species, we consistently captured the true value of CV, *S* and *K* of inter-individual variation in degree and overlap.

S.1.8 Nested patterns in individual-based plant-pollinator networks

We analyzed if the pollinator assemblages of specialist plant individuals were proper subsets of the pollinator assemblages of generalist individuals by estimating the nestedness (NODF,

Almeida-Neto et al. 2008) of the individual-based network within each plant species. To test whether there was evidence of nested patterns, we compared the observed NODF value to a distribution of NODF values (N= 1,000) obtained with a null model with constrained connectance and moderately constrained marginal totals ("vaznull" method, "bipartite" R package, Dormann et al. 2008).

S1.9 Feasibility of plant-pollinator communities

The feasibility of an equilibrium point corresponds to the conditions leading to positive abundances for all species occurring in a given community. Feasibility serves as an indicator of how much environmental stress a community can tolerate before extinction of any of its constituent species. It is defined as the volume of the parameter space of intrinsic growth rates in which all species in a community can have positive abundances. The size of the feasibility domain shows how much change in conditions can be tolerated by the community while all species remain extant. To calculate the feasibility of our plant-pollinator communities we used a generalized Lotka-Volterra model describing the population dynamics of species in a mutualistic network (Rohr et al. 2014; Saavedra et al. 2016, Song et al. 2018):

$$
\begin{cases}
\dfrac{dP_i}{dt} = P_i\left(r_i^{(P)} - \sum_j \alpha_{ij}^{(P)} P_j + \sum_j \gamma_{ij}^{(P)} A_j\right) \\
\dfrac{dA_i}{dt} = A_i\left(r_i^{(A)} - \sum_j \alpha_{ij}^{(A)} A_j + \sum_j \gamma_{ij}^{(A)} P_j\right)
\end{cases}
$$

where the variables P_i and A_i denote the abundance of plant and animal species i, respectively, r_i represents intrinsic growth rates, α_{ij} denotes the interspecific competition and γ_{ij} corresponds to the benefit received via mutualistic interactions. The mutualistic benefit is parameterized by $\gamma_{ij} = \gamma_0 y_{ij}/d_i^\delta$, where $y_{ij} = 1$ if species i and j interact and

zero otherwise; d_i is the number of interactions of species i; δ corresponds to the mutualistic trade-off (i.e., it modulates the extent to which a species that interacts with few other species does it strongly, whereas a species that interacts with many partners does it weakly; Saavedra et al. 2013); and γ_0 represents the overall level of mutualistic strength. For the competition parameters, a mean field approximation was used given the absence of empirical data on interspecific competition. We set $\alpha_{ii}^{(P)} = \alpha_{ii}^{(A)} = 1$ and $\alpha_{ij}^{(P)} = \alpha_{ij}^{(A)} = \rho(i \neq j)$ The mutualistic trade-off δ was set at 0.30. Results were qualitatively identical exploring values $0.01 < \delta < 0.5$. To focus on mutualistic effects, we ran analyses with zero interspecific competition ($\rho = 0$). The average mutualistic strength was set as half the average mutualistic strength at the stability threshold (see Simmons et al. 2020).

To calculate the community feasibility domain, a vector of intrinsic growth rates at the center of the feasibility domain is first estimated analytically. Because it is located at the center of the domain, this growth rate vector can tolerate the greatest changes before departing from the feasibility domain. The boundaries of the domain are then approximated by randomly perturbing this central intrinsic growth rate vector to measure the amount of deviation allowed before feasibility is lost (Rohr et al. 2014). The size of the feasibility domain is biased by the dimension of the community (Grilli et al. 2017), decreasing by increasing the community size. Therefore, we calculated the size of the feasibility domain by exponentiating the feasibility value by the inverse of the number of species in the community, as follows:

$$\omega(A) = \Omega(A)^{1/S}$$

Besides, we estimated the scaled value of the feasibility domain, so it ranges between 0 and 1.

References

Almeida-Neto, M., Guimaraes, P., Guimaraes Jr, P. R., Loyola, R. D., & Ulrich, W. (2008). A
consistent metric for nestedness analysis in ecological systems: reconciling concept
and measurement. *Oikos*, *117*(8), 1227-1239.

Dormann, C. F., Gruber, B., & Fründ, J. (2008). Introducing the bipartite package: analysing
ecological networks. *R News*, 8(2), 8-11.

Grilli, J., Adorisio, M., Suweis, S., Barabás, G., Banavar, J. R., Allesina, S., & Maritan, A.
(2017). Feasibility and coexistence of large ecological communities. *Nat. Commun.*,
8(1), 1-8.

Marquis, R. J. (1988). Phenological variation in the neotropical understory shrub Piper
arielanum: causes and consequences. *Ecology*, *69*(5), 1552-1565.

Rohr, R. P., Saavedra, S., & Bascompte, J. (2014). On the structural stability of mutualistic
systems. *Science*, *345*(6195), 1253497.

Saavedra, S., Rohr, R. P., Dakos, V., & Bascompte, J. (2013). Estimating the tolerance of
species to the effects of global environmental change. *Nat. Commun.*, *4*(1), 1-6.

Saavedra, S., Rohr, R. P., Olesen, J. M., & Bascompte, J. (2016). Nested species interactions
promote feasibility over stability during the assembly of a pollinator community.
Ecol. Evol., *6*(4), 997-1007.

Simmons, B. I., Wauchope, H. S., Amano, T., Dicks, L. V., Sutherland, W. J., & Dakos, V.
(2020). Estimating the risk of species interaction loss in mutualistic communities.
PLoS biology, *18*(8), e3000843.

Song, C., Rohr, R. P., & Saavedra, S. (2018). A guideline to study the feasibility domain of
multi-trophic and changing ecological communities. *J. Theor. Biol.*, *450*, 30-36.

Table S1. Number of individuals from each plant species sampled in each plot of the study area and total number of plant individuals sampled in all plots. In order to assess the completeness of sampling effort, we fitted the cumulative number of recorded pollinator morphotypes with increasing number of sampling days, calculating the Bootstrap asymptotic estimator. Sampling completeness values are indicated as the mean and standard deviation across all plant individuals within each species. For *Cistus salviifolius* and *Ulex australis* we could not calculate the sampling completeness as we did not manage to gather sufficient interaction data.

Plot	*Armeria velutina*	*Cistus libanotis*	*Cistus salviifolius*	*Halimium calycinum*	*Halimium halimifolium*	*Helichrysum picardii*	*Lavandula pedunculata*	*Salvia rosmarinus*	*Stauracanthus genistoides*	*Thymus mastichina*	*Ulex australis*
A	0	15	0	15	15	10	15	5	11	11	15
B	0	15	1	15	15	20	15	15	10	10	0
C	2	2	0	15	15	15	15	15	10	5	0
D	12	15	0	15	15	20	15	15	15	10	0
E	10	15	9	15	15	0	15	15	10	10	15
F	9	15	0	15	15	2	15	15	8	15	8
Total	33	77	10	90	90	67	90	80	64	61	38
Sampling completeness (mean ± SD)	92.10 ± 5.93	89.70 ± 5.75	NA	90.00 ± 6.27	87.60 ± 5.53	84.90 ± 4.82	94.90 ± 6.01	95.50 ± 4.47	94.80 ± 6.15	90.60 ± 5.23	NA

Table S2. List of pollinator taxa recorded at the study sites. Each row represents a pollinator morphotype. Note that pollinator morphotypes differ in the taxonomic resolution at which they were identified.

Order	Family	Genus	Species
Coleoptera	Buprestidae	Acmaeodera	NA
Coleoptera	Buprestidae	NA	NA
Coleoptera	Buprestidae	NA	NA
Coleoptera	Cantharidae	NA	NA
Coleoptera	Cantharidae	Malthodes	NA
Coleoptera	Cerambycidae	Deilus	NA
Coleoptera	Cerambycidae	Nustera	distigma
Coleoptera	Chrysomelidae	Chrysolina	americana
Coleoptera	Chrysomelidae	Coptocephala	NA
Coleoptera	Chrysomelidae	Tituboea	NA
Coleoptera	Coccinellidae	Exochomus	nigromaculatus
Coleoptera	Coccinellidae	Hyperaspis	NA
Coleoptera	Coccinellidae	Rhyzobius	lophanthae
Coleoptera	Coccinellidae	Scymnus	NA
Coleoptera	Curculionidae	NA	NA
Coleoptera	Curculionidae	Tychius	NA
Coleoptera	Dermestidae	Anthrenus	NA
Coleoptera	Dermestidae	Attagenus	NA
Coleoptera	Elateridae	Cardiophorus	NA
Coleoptera	Meloidae	Mylabris	NA
Coleoptera	Meloidae	Mylabris	NA
Coleoptera	Meloidae	Mylabris	NA
Coleoptera	Melyridae	Malachius	NA
Coleoptera	Mordellidae	NA	NA
Coleoptera	Mordellidae	NA	NA
Coleoptera	Mordellidae	NA	NA
Coleoptera	NA	NA	NA
Coleoptera	Nitidulidae	NA	NA
Coleoptera	Oedemeridae	Oedemera	NA
Coleoptera	Prionoceridae	Lobonyx	aeneus
Coleoptera	Scarabaeidae	Chasmatopterus	NA
Coleoptera	Tenebrionidae	Heliotaurus	ruficollis
Diptera	Bombyliidae	Bombylius	NA
Diptera	Bombyliidae	Exoprosopa	italica
Diptera	Bombyliidae	Lomatia	NA

Diptera	Bombyliidae	Phthiria	NA
Diptera	Bombyliidae	Phthiria	NA
Diptera	Bombyliidae	Phthiria	NA
Diptera	Bombyliidae	Usia	NA
Diptera	Bombyliidae	Usia	NA
Diptera	Calliphoridae	Rhyncomyia	cupraea
Diptera	NA	NA	NA
Diptera	NA	NA	NA
Diptera	NA	NA	NA
Diptera	NA	NA	NA
Diptera	NA	NA	NA
Diptera	NA	NA	NA
Diptera	NA	NA	NA
Diptera	NA	NA	NA
Diptera	NA	NA	NA
Diptera	NA	NA	NA
Diptera	NA	NA	NA
Diptera	Syrphidae	Episyrphus	balteatus
Diptera	Syrphidae	Episyrphus	NA
Diptera	Syrphidae	Eristalis	NA
Diptera	Syrphidae	Eupeodes	NA
Diptera	Syrphidae	Metasyrphus	corollae
Diptera	Syrphidae	Paragus	tibialis
Diptera	Syrphidae	Scaeva	NA
Diptera	Syrphidae	Sphaerophoria	scripta
Diptera	Syrphidae	Syritta	pipiens
Diptera	Syrphidae	NA	NA
Diptera	Syrphidae	NA	NA
Diptera	Syrphidae	NA	NA
Diptera	Syrphidae	NA	NA
Diptera	Syrphidae	NA	NA
Diptera	Syrphidae	NA	NA
Diptera	Syrphidae	NA	NA
Hymenoptera	Andrenidae	Andrena	NA
Hymenoptera	Anthophoridae	Thyreus	NA
Hymenoptera	Apidae	Amegilla	NA
Hymenoptera	Apidae	Anthophora	bimaculata
Hymenoptera	Apidae	Anthophora	NA
Hymenoptera	Apidae	Apis	mellifera
Hymenoptera	Apidae	Bombus	terrestris
Hymenoptera	Apidae	Ceratina	cucurbitina
Hymenoptera	Apidae	Ceratina	NA

Hymenoptera	Apidae	Eucera	NA
Hymenoptera	Apidae	Nomada	NA
Hymenoptera	Apidae	Xylocopa	cantabrita
Hymenoptera	Cabronidae	Bembix	flavescens
Hymenoptera	Cabronidae	Lindenius	luteiventris
Hymenoptera	Colletidae	Colletes	NA
Hymenoptera	Colletidae	Hylaeus	NA
Hymenoptera	Crabronidae	Diodontus	insidiosus
Hymenoptera	Halictidae	NA	NA
Hymenoptera	Halictidae	NA	NA
Hymenoptera	Halictidae	NA	NA
Hymenoptera	Halictidae	Halictus	NA
Hymenoptera	Halictidae	Halictus	NA
Hymenoptera	Halictidae	Halictus	NA
Hymenoptera	Halictidae	Lasioglossum	NA
Hymenoptera	Halictidae	Lasioglossum	NA
Hymenoptera	Halictidae	Lasioglossum	NA
Hymenoptera	Halictidae	Lasioglossum	NA
Hymenoptera	Halictidae	Lasioglossum	NA
Hymenoptera	Halictidae	Lasioglossum	NA
Hymenoptera	Megachilidae	Anthidiellum	strigatum
Hymenoptera	Megachilidae	Chalicodoma	sicula
Hymenoptera	Megachilidae	Chelostoma	NA
Hymenoptera	Megachilidae	Heriades	NA
Hymenoptera	Megachilidae	Megachile	apicalis
Hymenoptera	Megachilidae	Megachile	sicula
Hymenoptera	Megachilidae	Megachile	NA
Hymenoptera	Megachilidae	NA	NA
Hymenoptera	Megachilidae	Osmia	NA
Hymenoptera	Melittidae	Dasypoda	NA
Hymenoptera	NA	NA	NA
Hymenoptera	Tiphiidae	Meria	tripunctata
Hymenoptera	Tiphiidae	Tiphia	morio
Hymenoptera	Vespidae	Ancistrocerus	NA
Hymenoptera	Vespidae	NA	NA
Hymenoptera	Vespidae	Vespula	NA
Lepidoptera	Lycaenidae	Laeosopis	roboris
Lepidoptera	Lycaenidae	Lycaena	phlaeas
Lepidoptera	Lycaenidae	Plebejus	argus
Lepidoptera	Microlepidoptera (artificial)	NA	NA
Lepidoptera	Nymphalidae	Pyronia	cecilia
Lepidoptera	Nymphalidae	Nymphalis	polychloros
Lepidoptera	Sphingidae	Macroglossum	stellatarum

Table S3. Number of pollinator taxa identified within each order, total number of visits to plant individuals and percentage of the total number of visits recorded. Pollinator morphotypes were identified at the species (27.27%), genus (44.63%), family (16.53%) and order (11.57%) levels. Previous independent surveys in our study area showed that only one to three species with very similar morphology and behavior occur within each of the lumped genera or families.

Order	Number of taxa	Number of visits	% Total visits
Hymenoptera (Apoidea)	37	22926	65.90
Coleoptera	32	7678	22.10
Diptera	37	3246	9.33
Lepidoptera	7	718	2.06
Hymenoptera (non Apoidea)	8	207	0.60
Total	121	34775	100

Table S4. Nestedness (NODF) estimated for the individual-based plant-pollinator network of each plant species. The z-cores and *P* value were estimated by comparing the observed value to a distribution of values (N=1,000) obtained with a null model (Appendix S1.8) with constrained connectance and moderately constrained marginal totals.

	NODF z-score	P
Armeria velutina	2.09	0.02
Cistus libanotis	5.89	<0.001
Halimium calycinum	5.61	<0.001
Halimium halimifolium	6.95	<0.001
Helichrysum picardii	3.84	<0.001
Lavandula pedunculata	1.80	0.03
Salvia rosmarinus	4.91	<0.001
Stauracanthus genistoides	2.69	0.01
Thymus mastichina	6.56	<0.001

Table S5. Results from the linear mixed models testing the effects of plant attributes on the degree (i.e., number of pollinator morphotypes used) of plant individuals for the different species.

Coefficient	AVEL Estimates	AVEL Conf. Int (95%)	AVEL P-Value	CLIB Estimates	CLIB Conf. Int (95%)	CLIB P-Value	HCOM Estimates	HCOM Conf. Int (95%)	HCOM P-Value	HHAL Estimates	HHAL Conf. Int (95%)	HHAL P-Value	HPIC Estimates	HPIC Conf. Int (95%)	HPIC P-Value	LPED Estimates	LPED Conf. Int (95%)	LPED P-Value	ROFF Estimates	ROFF Conf. Int (95%)	ROFF P-Value	SGEN Estimates	SGEN Conf. Int (95%)	SGEN P-Value	TMAS Estimates	TMAS Conf. Int (95%)	TMAS P-Value
Intercept	0.00	-0.10 – 0.09	0.93	0.01	-0.08 – 0.10	0.84	0.01	-0.06 – 0.08	0.87	0.07	-0.06 – 0.20	0.32	0.03	-0.21 – 0.14	0.7	0.12	-0.06 – 0.19	**<0.001**	-0.01	-0.11 – 0.10	0.9	0.1	-0.02 – 0.17	**0.02**	-0.01	-0.09 – 0.08	0.88
Number of flowers	0.4	0.23 – 0.57	**<0.001**	0.11	-0.04 – 0.26	0.15	0.08	-0.00 – 0.17	**0.05**	0.12	-0.00 – 0.25	**0.05**	0.31	0.18 – 0.44	**<0.001**	0.26	0.15 – 0.37	**<0.001**	0.18	0.05 – 0.32	**0.01**	0.09	-0.03 – 0.20	0.14	0.07	-0.02 – 0.16	0.11
Conspecific flowering synchrony	0.02	-0.09 – 0.13	0.66	0.08	-0.05 – 0.20	0.22	0.1	-0.01 – 0.20	**0.03**	-0.06	-0.18 – 0.06	0.33	0.16	-0.02 – 0.34	0.08	0.01	-0.08 – 0.06	0.71	0.2	-0.08 – 0.33	**<0.001**	0.07	-0.04 – 0.19	0.21	0.08	-0.00 – 0.16	**0.05**
Heterospecific flowering synchrony	0.04	-0.07 – 0.14	0.48	0.04	-0.04 – 0.12	0.36	0.03	-0.09 – 0.03	0.32	0.09	-0.01 – 0.20	0.09	0.09	-0.18 – 0.00	0.06	0.06	-0.12 – -0.00	**0.04**	-0.13	-0.21 – -0.05	**<0.001**	-0.04	-0.10 – 0.02	0.21	0	-0.05 – 0.05	0.97
Conspecific neighborhood cover	-0.01	-0.13 – 0.12	0.9	-0.09	-0.20 – 0.02	0.1	-0.01	-0.08 – 0.05	0.69	-0.03	-0.15 – 0.09	0.57	-0.02	-0.15 – 0.12	0.8	-0.05	-0.01 – 0.11	0.09	-0.08	-0.16 – 0.00	0.05	0	-0.06 – 0.06	0.99	0	-0.08 – 0.08	0.92
Heterospecific neighborhood cover	0.07	-0.06 – 0.20	0.29	0.05	-0.04 – 0.14	0.27	0.01	-0.08 – 0.07	0.89	0.08	-0.06 – 0.22	0.25	0.04	-0.08 – 0.16	0.52	0.01	-0.08 – 0.05	0.69	0.02	-0.06 – 0.10	0.66	-0.07	-0.14 – -0.00	**0.05**	0.05	-0.02 – 0.12	0.19
R²	0.518			0.149			0.115			0.090			0.311			0.311			0.248			0.168			0.136		

Table S6. Results from the linear mixed models testing the effects of plant attributes on the niche overlap (i.e., overlap in pollinator use with conspecifics) of plant individuals for the different species.

Coefficient	AVEL Estimate	AVEL CI (95%)	AVEL P-Value	CLIB Estimate	CLIB CI (95%)	CLIB P-Value	HCOM Estimate	HCOM CI (95%)	HCOM P-Value	HHAL Estimate	HHAL CI (95%)	HHAL P-Value	HPIC Estimate	HPIC CI (95%)	HPIC P-Value	LPED Estimate	LPED CI (95%)	LPED P-Value	ROFF Estimate	ROFF CI (95%)	ROFF P-Value	SGEN Estimate	SGEN CI (95%)	SGEN P-Value	TMAS Estimate	TMAS CI (95%)	TMAS P-Value
Intercept	0.3	-0.03 – 0.63	0.07	0.17	-0.10 – 0.44	0.2	0.16	-0.10 – 0.42	0.23	0.13	-0.10 – 0.36	0.26	0.28	-0.06 – 0.61	0.1	0.61	0.40 – 0.81	**<0.001**	0.14	-0.12 – 0.40	0.28	0.45	0.20 – 0.70	**<0.001**	0.51	0.24 – 0.78	**<0.001**
Number of flowers	0.1	-0.47 – 0.66	0.73	0.2	-0.24 – 0.64	0.37	0.38	0.07 – 0.69	**0.02**	0.38	0.15 – 0.60	**<0.001**	0.17	-0.08 – 0.41	0.18	0.22	-0.12 – 0.55	0.2	0.32	-0.01 – 0.66	0.06	-0.03	-0.40 – 0.34	0.86	0.23	-0.05 – 0.52	0.1
Conspecific flowering synchrony	0.23	-0.13 – 0.60	0.2	0.26	-0.11 – 0.63	0.17	0.55	0.19 – 0.90	**<0.001**	0.33	0.11 – 0.55	**<0.001**	0.56	0.22 – 0.89	**<0.001**	-0.07	-0.28 – 0.15	0.53	0.71	0.40 – 1.02	**<0.001**	0.36	-0.01 – 0.74	0.06	0.02	-0.28 – 0.23	0.86
Heterospecific flowering synchrony	-0.05	-0.39 – 0.29	0.76	0.18	-0.06 – 0.43	0.14	-0.29	-0.52 – -0.06	**0.01**	-0.01	-0.20 – 0.18	0.89	-0.26	-0.43 – -0.09	**<0.001**	0.11	-0.29 – 0.08	0.27	-0.4	-0.59 – -0.20	**<0.001**	-0.12	-0.32 – 0.08	0.25	-0.05	-0.22 – 0.12	0.53
Conspecific neighborhood cover	-0.02	-0.43 – 0.40	0.94	-0.16	-0.49 – 0.17	0.34	-0.01	-0.25 – 0.26	0.96	-0.21	-0.42 – 0.00	0.05	-0.05	-0.31 – 0.20	0.69	-0.04	-0.21 – 0.14	0.69	0	-0.21 – 0.21	1	-0.01	-0.21 – 0.18	0.88	-0.14	-0.12 – 0.39	0.28
Heterospecific neighborhood cover	0.09	-0.34 – 0.53	0.66	0.04	-0.24 – 0.32	0.77	-0.02	-0.29 – 0.24	0.87	0.09	-0.15 – 0.34	0.44	-0.12	-0.35 – 0.11	0.29	0.05	-0.17 – 0.26	0.66	-0.04	-0.23 – 0.16	0.72	-0.3	-0.52 – -0.09	**0.01**	0.02	-0.21 – 0.26	0.85
R^2	0.090			0.163			0.176			0.260			0.264			0.073			0.279			0.180			0.062		

Figure S1. Insect-pollinated shrub species (A-H) occurring in the study sites (L) located in Doñana National Park. A- *Halimium halimifolium*, B- *Helichrysum picardii*, C- *Armeria velutina*, D- *Cistus libanotis*, E- *Ulex australis*, F- *Stauracanthus genistoides*, G- *Thymus mastichina*, H- *Cistus salviifolius*, I- *Halimium calycinum*, J- *Lavandula pedunculata*, K- *Salvia rosmarinus*. *Cistus salviifolius* (H) and *Ulex australis* (E) were excluded from our analyses due to an extremely low abundance in the study sites and a very early flowering period, respectively.

Figure S2. Phenology of the co-occurring shrub species (B) on the study sites and the major pollinator groups visiting those species (A) across the flowering season (early February to mid-July). The width of each curve is proportional to the number of flowers produced (B) and the number of pollinator visits recorded (A).

A
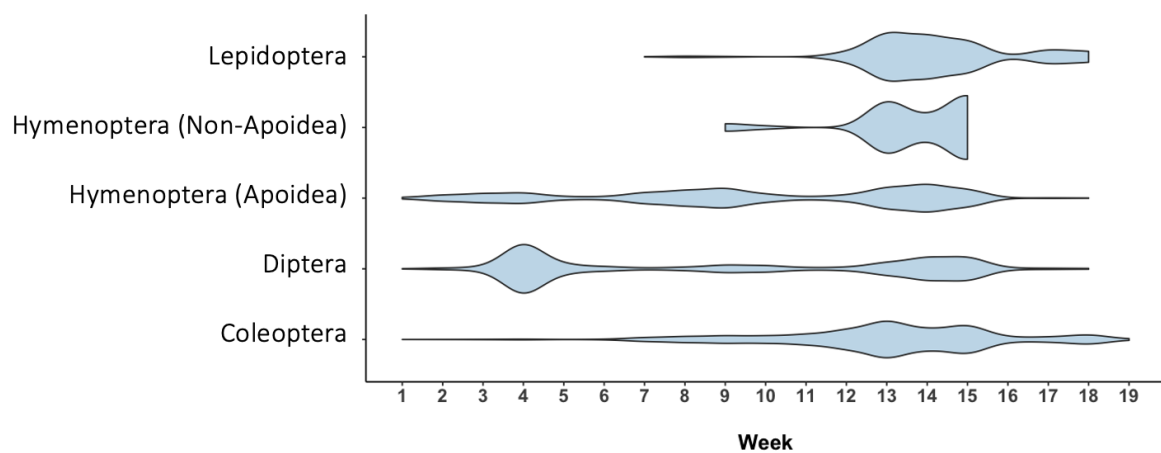
B
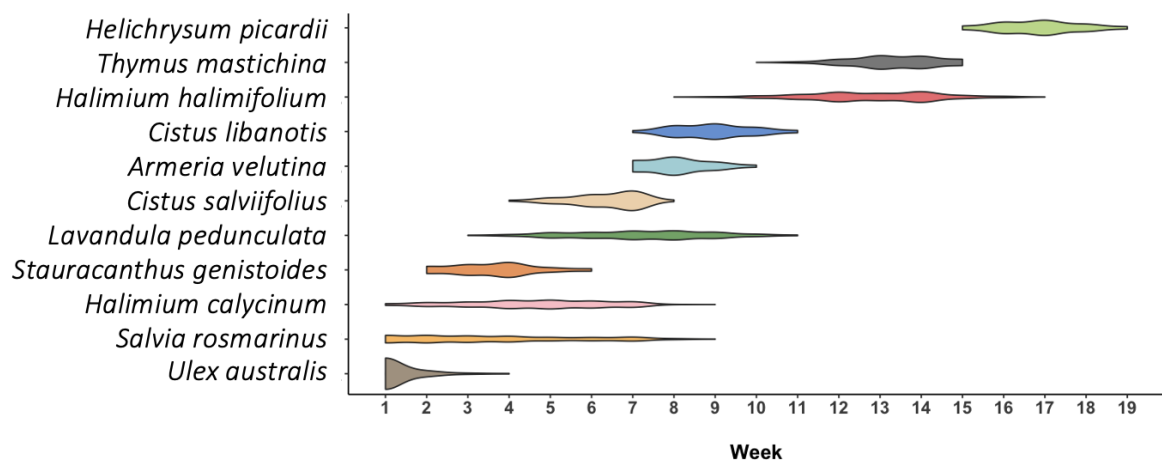
Figure S3. Spatial distribution of plant individuals belonging to different species (colors) in one plot of the study area.
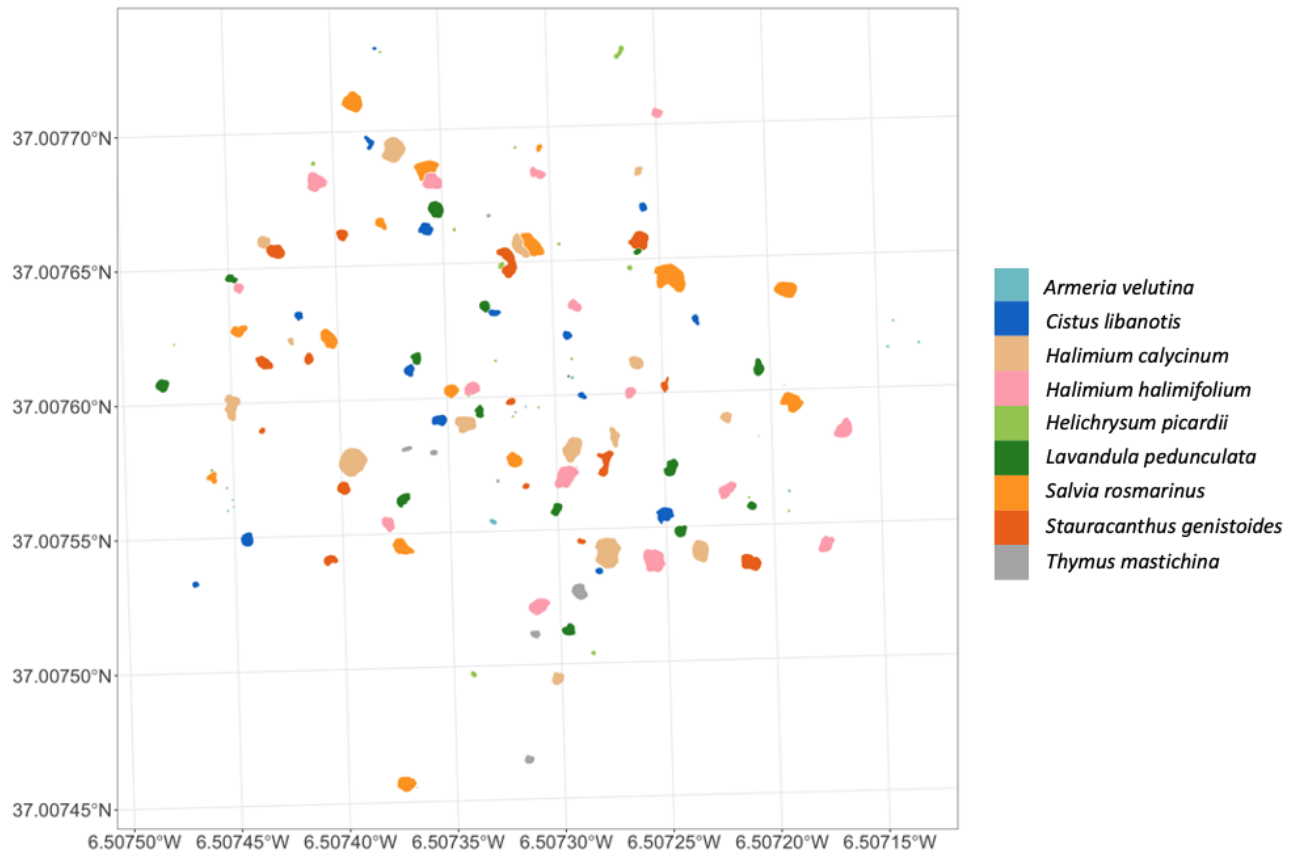
Fig S4. Coefficient of variation, skewness and kurtosis of the distribution of individual values of degree (i.e., number of pollinator morphotypes used) and niche overlap (i.e., overlap in pollinator use with conspecifics) for all plant species. A significant high kurtosis (>3) characterizes a peaked distribution, indicating a large number of plant individuals with similar roles in the population. A low kurtosis (<3) represents a flatter and more even distribution of individual roles (i.e., there are many plant individuals displaying different roles). Significant negative or positive skewness values occur when the distributions of plant individuals' roles are strongly left- or right-tailed, respectively, with a few plant individuals that play extreme roles compared with the bulk of the distribution. Values that depart from those expected in a normal distribution (kurtosis= 3 and skewness= 0 indicated with dashed gray lines) are represented by * ($P< 0.05$), ** ($P< 0.01$) and *** ($P< 0.001$).
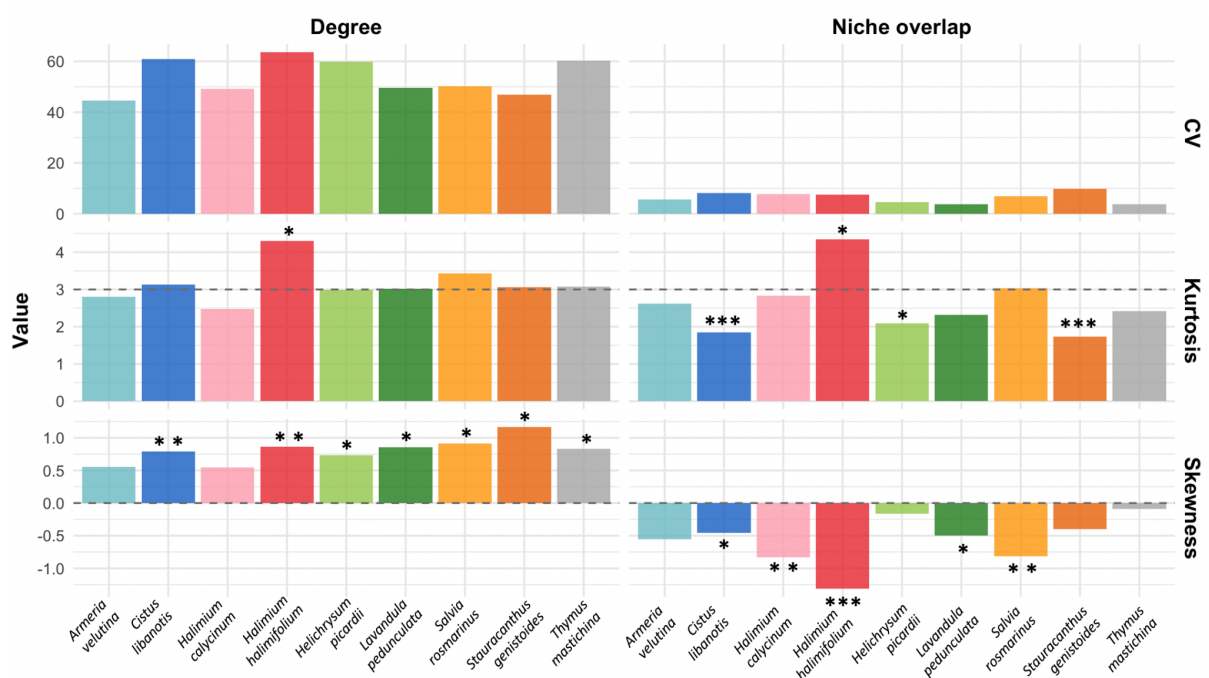
Fig. S5. Coefficient of variation (CV), skewness and kurtosis of degree (i.e., number of pollinator morphotypes used) and niche overlap (i.e., overlap in pollinator use with conspecifics) over an increasing number of individuals in the individual-based plant-pollinator network within each plant species. The solid line represents the mean coefficient of variation in individual-level topological metrics across 100 resampled networks created by randomly sampling a different subset of individuals within each species. The shaded area around the line indicates the standard deviation across all randomizations.
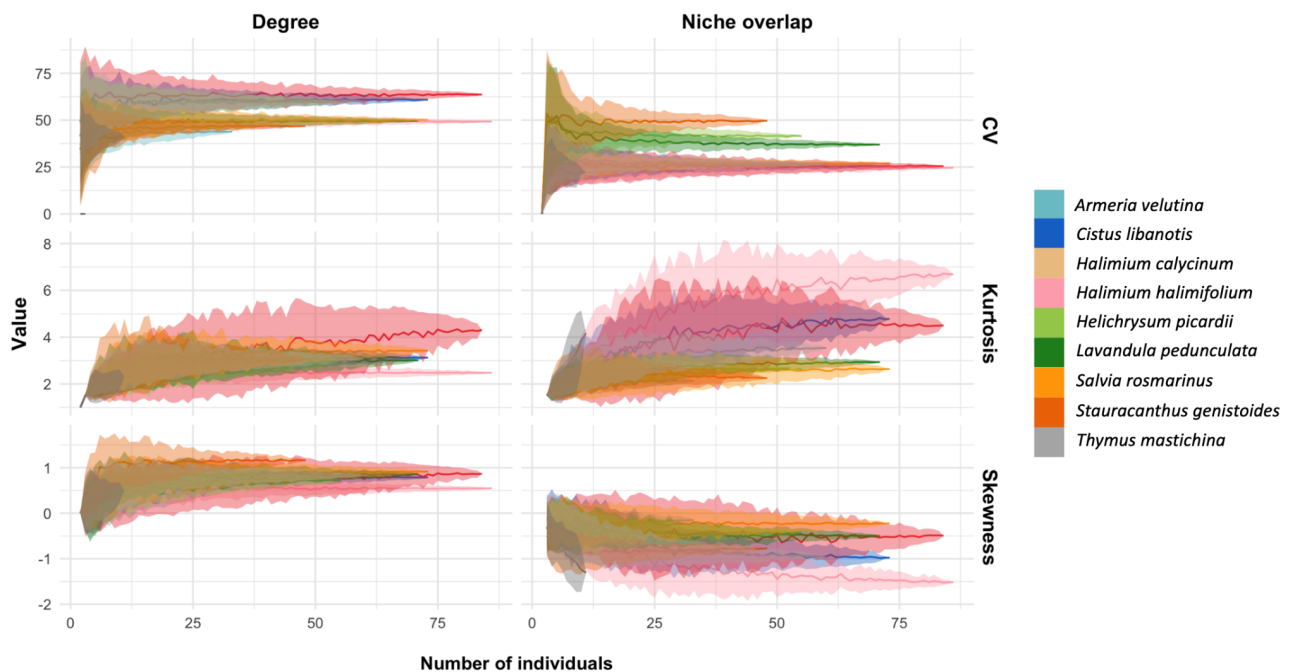
Figure S6. Results from linear models analyzing the effects of plant attributes on the plant individuals' degree (i.e., number of pollinator morphotypes used) and niche overlap (i.e., overlap in pollinator use with conspecifics) from different species (colors). Plant attributes are considered to have significant effects on a topological metric provided the confidence interval (whiskers) of the coefficient estimates (dots) do not contain zero. For flowering synchrony and neighborhood cover, C indicates conspecific, and H stands for heterospecific.
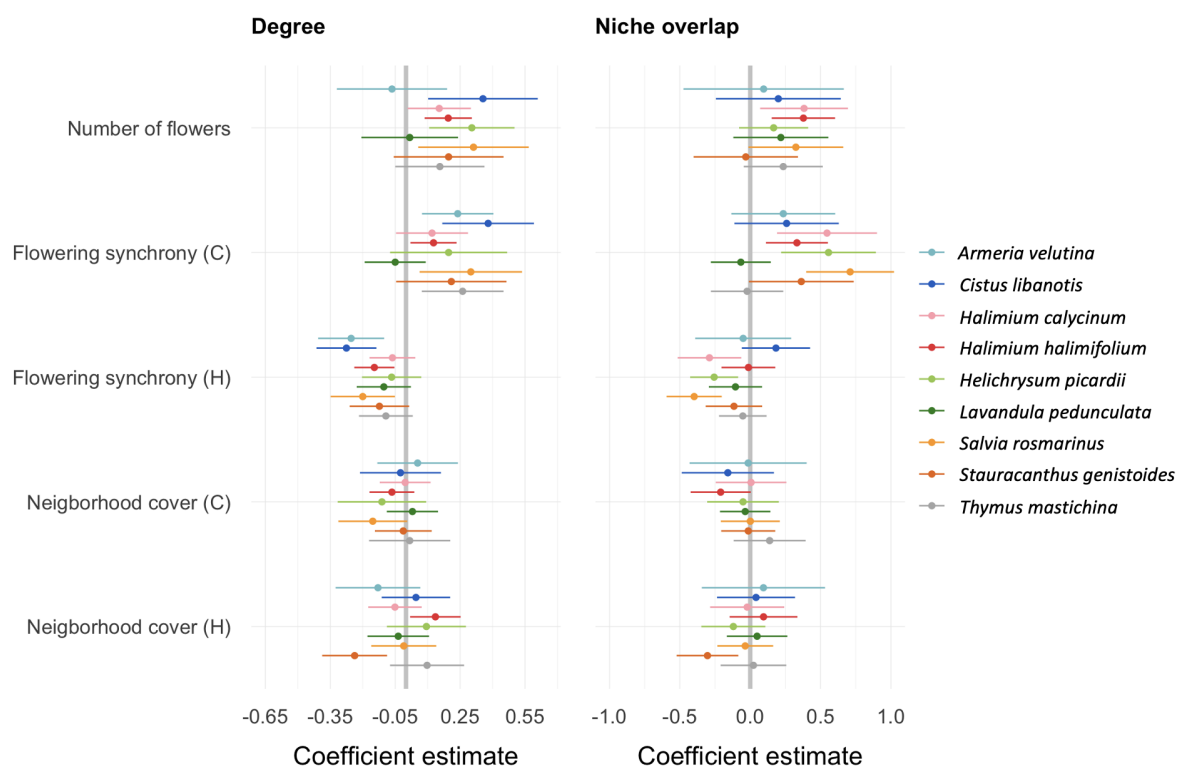
Figure S7. Total number of flowers produced per plant individual (A) and coefficient of variation (i.e., inter-individual variation) in the number of flowers produced per plant individual (B) in different sets of resampled interaction networks. The "random" set represents networks containing a combination of plant individuals with different levels of flower production (i.e., higher inter-individual variation). The "lower tercile", "middle tercile" and "upper tercile" sets represent networks with lower inter-individual variation in flower production, containing plant individuals within the lower, middle and upper tercile of flower production, respectively. Within each set we generated 100 species-based plant-pollinator networks by randomly selecting 100 plant individuals distributed among plant species proportionally to their relative abundance and summing the interactions established by these plant individuals at the species level. The solid line represents the mean. The total number of flowers per individual was previously scaled to range between 0 and 1 within each species to be standardized across all plant species.
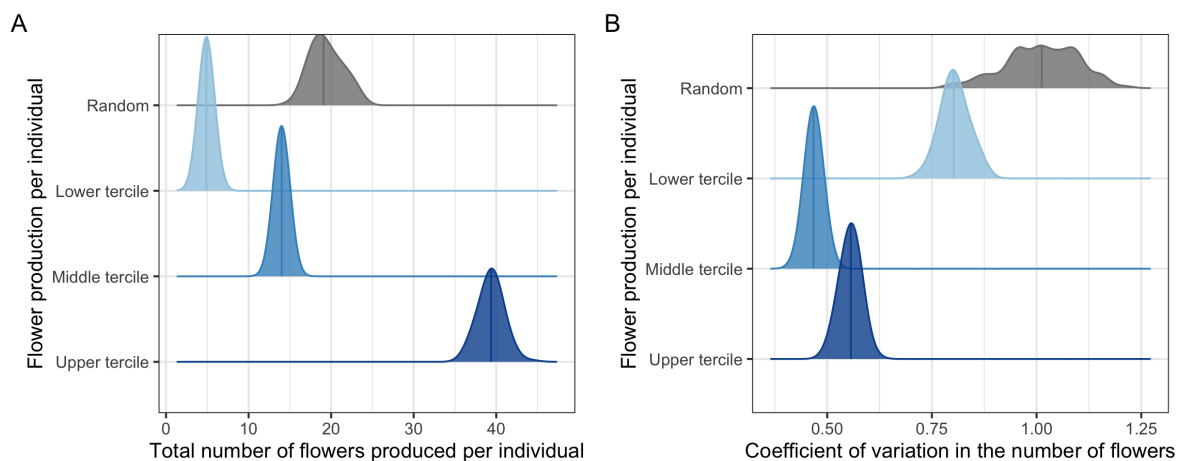
Figure S8. Changes in community-level network nestedness (NODF) with an increasing number of pollinator morphotypes. The "random" set represents networks containing a combination of plant individuals with different levels of flower production (i.e., higher inter-individual variation). The "lower tercile", "middle tercile" and "upper tercile" sets represent networks with lower inter-individual variation in flower production, containing plant individuals within the lower, middle and upper tercile of flower production, respectively. Within each set we generated 100 species-based plant-pollinator networks by randomly selecting 100 plant individuals distributed among plant species proportionally to their relative abundance and summing the interactions established by these plant individuals at the species level. The number of pollinator morphotypes in each resampled network can change as a result of the differences in the pollinator assemblage of the 100 individual plants randomly selected. The shaded area around the line indicates the 95% confidence interval of the linear regression across all randomizations.
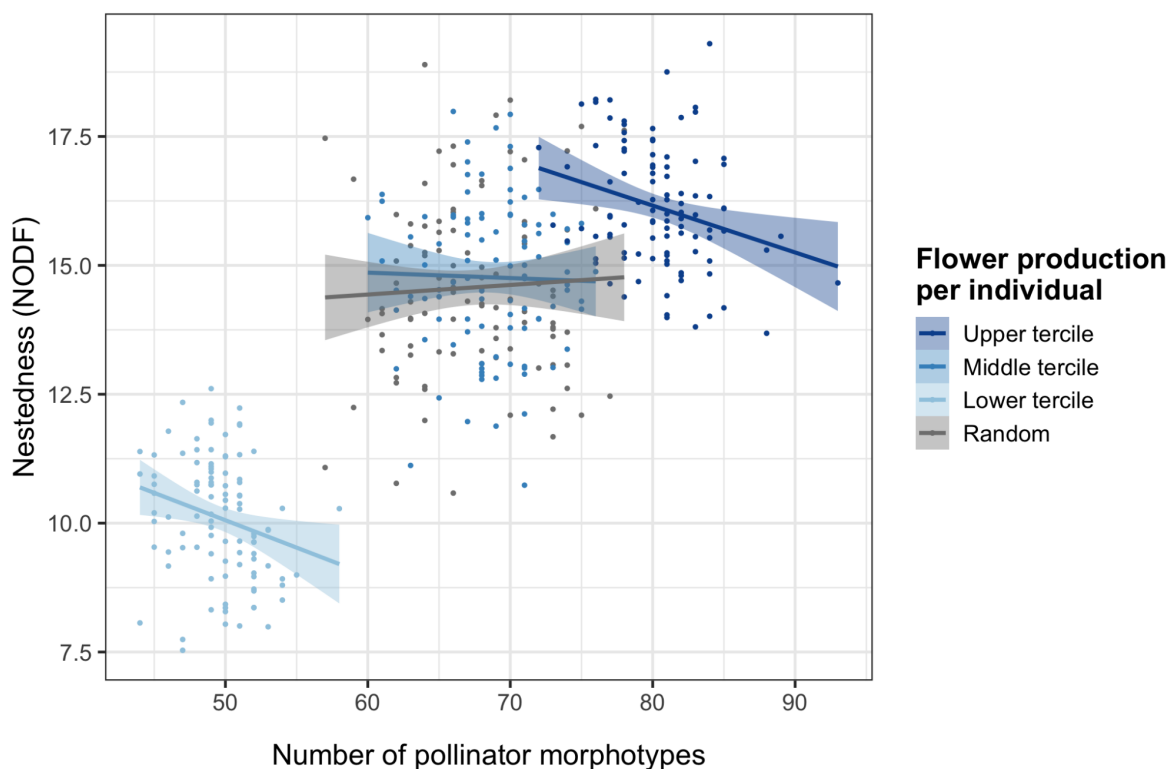
Figure S9. Changes in plant species-level degree (i.e., number of pollinator morphotypes used), overlap among plant species in pollinator use, community-level network nestedness and community feasibility across increasing community sizes (i.e., total number of plant individuals included in the community). The "random" set represents networks containing a combination of plant individuals with different levels of flower production (i.e., higher inter-individual variation). The "lower tercile", "middle tercile" and "upper tercile" sets represent networks with lower inter-individual variation in flower production, containing plant individuals within the lower, middle and upper tercile of flower production, respectively. Within each set we generated 100 species-based plant-pollinator networks by randomly selecting 100 plant individuals distributed among plant species proportionally to their relative abundance and summing the interactions established by these plant individuals at the species level. The solid line represents the mean across the 100 resampled networks. The shaded area around the line indicates the standard deviation across all randomizations.